

Heterometal Substitution in the Dimensional Reduction of Cluster Frameworks: Synthesis of Soluble $[\text{Re}_{6-n}\text{Os}_n\text{Se}_8\text{Cl}_6]^{(4-n)-}$ ($n = 1-3$) Cluster-Containing Solids

Eric G. Tulsy and Jeffrey R. Long*

Department of Chemistry, University of California, Berkeley, California 94720-1460

Received August 10, 2001

A general method for deconstructing cluster frameworks via heterometal substitution is demonstrated with application to the two-dimensional phase $\text{Re}_6\text{Se}_8\text{Cl}_2$. Solid-state reactions intended to replace two of the Re^{III} centers in the parent compound with $\text{Os}^{\text{IV}}\text{Cl}$ units indeed yield $\text{Re}_4\text{Os}_2\text{Se}_8\text{Cl}_4$. The crystal structure of this new phase reveals a less tightly connected two-dimensional framework, wherein face-capped octahedral $[\text{Re}_4\text{Os}_2\text{Se}_8]^{4+}$ cluster cores are linked through μ_2 -chloride bridges in one dimension and unsupported metal–selenium bonds in the other. Use of CsCl as a standard dimensional reduction agent in conjunction with heterometal substitution affords $\text{Cs}_3\text{Re}_5\text{OsSe}_8\text{Cl}_6$ and $\text{Cs}_2\text{Re}_4\text{Os}_2\text{Se}_8\text{Cl}_6$, soluble salts containing discrete molecular clusters. Reactions employing KCl and targeting a triosmium cluster further produce the soluble mixed-cluster salt $\text{K}_2[\text{Re}_3\text{Os}_3\text{Se}_8\text{Cl}_6][\text{Re}_4\text{Os}_2\text{Se}_7\text{Cl}_7]$. FT-ICR mass spectra confirm the presence of $[\text{Re}_{6-n}\text{Os}_n\text{Se}_8\text{Cl}_6]^{(4-n)-}$ ($n = 1-3$) clusters in solutions of these solids. Metathesis reactions supply $(\text{Bu}_4\text{N})_3[\text{Re}_5\text{OsSe}_8\text{Cl}_6]$ and $(\text{Bu}_4\text{N})_2[\text{Re}_4\text{Os}_2\text{Se}_8\text{Cl}_6]$, which then react with PEt_3 under forcing conditions to give $[\text{Re}_5\text{OsSe}_8(\text{PEt}_3)_6]^{3+}$ and $[\text{Re}_4\text{Os}_2\text{Se}_8(\text{PEt}_3)_6]^{4+}$ in high yield. Analysis of the latter diosmium species by ^{31}P NMR spectroscopy indicates a mixture of isomers, in which 55% of the clusters have the osmium atoms disposed trans to each other, while the remainder adopt the alternative cis configuration. Cyclic voltammetry measurements reveal a reversible one-electron reduction for $[\text{Re}_5\text{OsSe}_8\text{Cl}_6]^{3-}$ and multiple one-electron reductions for the mono- and diosmium hexaphosphine clusters; in the latter case, the trans isomer is observed to be more easily reduced than the cis isomer. Electronic structure calculations utilizing density functional theory show the trans isomer of $[\text{Re}_4\text{Os}_2\text{Se}_8\text{Cl}_6]^{2-}$ to be 4.5 kcal/mol more stable than the cis isomer, in approximate agreement with the observed ratio of reaction products. Moreover, the calculations expose significant differences in the contributions of rhenium and osmium to the frontier orbitals of the clusters, suggesting the possibility of observing metal-selective reactivity. An initial example of such behavior is provided with the synthesis of trans,trans- $[\text{Re}_4\text{Os}_2\text{Se}_8(\text{PEt}_3)_2\text{Cl}_4]$, wherein PEt_3 ligands preferentially bind the osmium centers.

Introduction

Dimensional reduction has been set forth as a general method for attempting to dismantle extended metal–anion ($\text{M}-\text{X}$) frameworks in a predictive manner.^{1,2} In such a reaction, a binary parent compound MX_x is heated with n equivalents of a dimensional reduction agent A_nX (where A is significantly more electropositive than M), to form a ternary child compound $\text{A}_{n\alpha}\text{MX}_{x+n}$ with fewer $\text{M}-\text{X}-\text{M}$ bridging interactions. Thus, for example, dimensional reduction of a two-dimensional MX_4 framework³ might be expected to produce the lower-dimensional phases depicted in Figure 1.⁴ This preparative technique has also proven effective in dismantling extended frameworks comprised of interlinked transition metal clusters.^{1,5} As an illustrative example, consider the compound $\text{Mo}_6\text{Cl}_{12}$ ($=[\text{Mo}_6\text{Cl}^{\text{I}}_8\text{Cl}^{\text{II}}_2\text{Cl}^{\text{III}}_2]^{4-}$),^{6,7} which adopts a structure related to the MX_4 structure simply by replacing each M^{4+} metal ion with an

$[\text{Mo}_6\text{Cl}_8]^{4+}$ cluster core (see Figure 1). Dimensional reduction of this compound proceeds in a manner analogous to that of MX_4 , affording one-dimensional chains, as observed in $\text{NaMo}_6\text{Cl}_{13}$ ($=\text{Na}[\text{Mo}_6\text{Cl}^{\text{I}}_8\text{Cl}^{\text{II}}_4\text{Cl}^{\text{III}}_1]^{4-}$),⁸ and discrete molecular clusters, as observed in $\text{Cu}_2\text{Mo}_6\text{Cl}_{14}$ ($=\text{Cu}_2[\text{Mo}_6\text{Cl}^{\text{I}}_8\text{Cl}^{\text{II}}_6]^{4-}$).⁹ The method has further been applied in dismantling $\text{Re}_6\text{Se}_8\text{Cl}_2$ ($=[\text{Re}_6\text{Se}_4\text{Se}^{\text{I}}_4\text{Se}^{\text{II}}_4\text{Cl}^{\text{III}}_2]^{4-}$), a two-dimensional solid with a dense eight-connected framework wherein face-capped octahedral $[\text{Re}_6\text{Se}_8]^{2+}$ cluster cores are directly linked through rhombic Re_2Se_2 interactions.¹⁰ High-temperature reactions incorporating ACl disconnect this otherwise intractable phase to give related compounds with less tightly connected frameworks (as specified in the leftmost column of Scheme 1).⁵ Such reactions have led to soluble $[\text{Re}_6\text{Q}_8]^{2+}$ ($\text{Q} = \text{S}, \text{Se}$) core-containing clusters that cannot be prepared by more traditional self-assembly or excision¹¹ routes, permitting access to a new realm of solution chemistry.¹²

(1) Tulsy, E. G.; Long, J. R. *Chem. Mater.* **2001**, *13*, 1149.

(2) A related relationship between alkali metal incorporation and dimensionality was noted for specific metal chalcogenides in: (a) Kanatzidis, M. G.; Park, Y. *Chem. Mater.* **1990**, *2*, 99. (b) Lu, Y.-J.; Ibers, J. A. *Comments Inorg. Chem.* **1993**, *14*, 229. (c) Axtell, E. A., III; Liao, J.-H.; Pikramenou, Z.; Park, Y.; Kanatzidis, M. G. *J. Am. Chem. Soc.* **1993**, *115*, 12191.

(3) The particular framework shown is taken from the crystal structure of VF_4 : Cretenet, J.-C. *Rev. Chim. Miner.* **1973**, *10*, 399.

(4) It is important to note that, since the presumed child compounds are thermodynamically stable products of high temperature reactions, dimensional reduction need not be carried out in the stepwise fashion depicted but rather can be employed in directly targeting compounds with the desired structural attributes.

(5) (a) Long, J. R.; Williamson, A. S.; Holm, R. H. *Angew. Chem., Int. Ed. Engl.* **1995**, *34*, 226. (b) Long, J. R.; McCarty, L. S.; Holm, R. H. *J. Am. Chem. Soc.* **1996**, *118*, 4603.

(6) Here we use the Schäfer notation for distinguishing between inner (i) and outer (a, ausser) ligands:^{5b} Schäfer, H.; von Schnering, H. G. *Angew. Chem.* **1964**, *76*, 833.

(7) von Schnering, H. G.; May, W.; Peters, K. Z. *Kristallogr.* **1993**, *208*, 368.

(8) Boesch, S.; Keller, H.-L. Z. *Kristallogr.* **1991**, *196*, 159.

(9) Peppenhorst, A.; Keller, H.-L. Z. *Anorg. Allg. Chem.* **1996**, *622*, 663.

(10) Leduc, P. L.; Perrin, A.; Sergent, M. *Acta Crystallogr.* **1983**, *C39*, 1503.

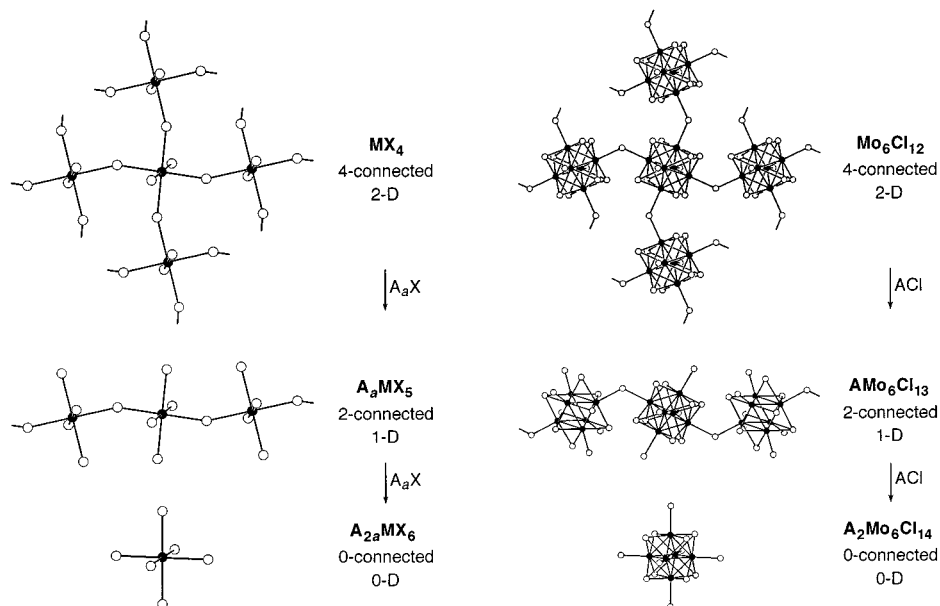


Figure 1. Left: Dimensional reduction of an MX_4 framework.^{3,4} M atoms (represented by black spheres) are octahedrally coordinated by X atoms (white spheres). Reaction with A_aX incorporates additional X atoms into the M–X framework, terminating M–X–M bridges to reduce the connectedness and dimensionality of the framework. Right: Dimensional reduction of $\text{Mo}_6\text{Cl}_{12}$.^{4,7} Cluster cores formed from six Mo atoms (represented by black spheres) and eight Cl atoms (white spheres) are connected through outer chloride ligands in $\text{Mo}_6\text{Cl}_{12}$. Incorporation of additional chloride ligands terminates intercluster bridges to give one-dimensional chains and discrete molecular clusters.

Cluster–anion frameworks provide a controllable parameter not present in simple metal–anion frameworks, since the composition of the cluster core can be varied. Through appropriate isoelectronic substitutions, the charge needed to counterbalance additional bridge-terminating anions can be placed on the cluster itself rather than on external counterions.¹³ This alternate method for formulating dimensionally reduced compounds also succeeds in disconnecting $\text{Re}_6\text{Se}_8\text{Cl}_2$. Thus, substitution of Cl^- for Se^{2-} in the cluster core compensates for incorporation of additional apical chloride ligands in the $(8 - 2n)$ -connected child compounds $[\text{Re}_6\text{Se}_{8-n}\text{Cl}_n]\text{Cl}_{2+n}$ ($n = 1-4$),¹⁴ as shown along the horizontal axis in Scheme 1. Each successive

replacement results in a less tightly connected framework with more positively charged cluster cores, until finally the discrete molecular cluster $\text{Re}_6\text{Se}_4\text{Cl}_{10}$ ($=[\text{Re}_6\text{Se}_4\text{Cl}_4]\text{Cl}_6$) is formed. Combining this substitutional method with standard dimensional reduction then begets the two-dimensional array of potential target compounds enumerated in Scheme 1. Similar disconnecting substitutions are apparent in a few other systems, most notably with variation of the interstitial element in centered zirconium chloride clusters accompanying incorporation of additional outer chloride ligands in the following series: $\text{Zr}_6\text{BeCl}_{12}$, $\text{Zr}_6\text{BCl}_{13}$, $\text{Zr}_6\text{CCl}_{14}$, $\text{Zr}_6\text{NCl}_{15}$.¹⁶

Another form of isoelectronic replacement that could potentially be utilized in dismantling cluster frameworks involves substitution of a heterometal atom. Hexanuclear mixed-metal clusters have been reported in the Chevrel-type phases $\text{Mo}_{6-x}\text{M}_x\text{Q}_8$ ($\text{M} = \text{Re}, \text{Q} = \text{S}, \text{Se}, \text{Te}, x = 4; \text{M} = \text{Ru}, \text{Q} = \text{Se}, \text{Te}, 0 \leq x \leq 2; \text{M} = \text{Rh}, \text{Q} = \text{Te}, x = 0.5, 1.33$)¹⁷ and $\text{Nb}_{6-x}\text{Ru}_x\text{Te}_8$ ($2.50 \leq x \leq 3.17$).¹⁸ However, the electron count for the clusters present in these compounds is seen to be quite variable, such that the substitutions result in reduction of the framework rather than incorporation of additional anions. In contrast, compounds containing Re_6Q_8 type clusters exhibit a strong preference for compositions with a precise count of 24 metal-based valence electrons (corresponding to one bonding pair per edge of the Re_6 octahedron), suggesting that heterometal

(11) Lee, S. C.; Holm, R. H. *Angew. Chem., Int. Ed. Engl.* **1990**, *29*, 840 and references therein.

(12) (a) Zheng, Z.; Long, J. R.; Holm, R. H. *J. Am. Chem. Soc.* **1997**, *119*, 2163. (b) Zheng, Z.; Holm, R. H. *Inorg. Chem.* **1997**, *36*, 5173. (c) Willer, M. W.; Long, J. R.; McLauchlan, C. C.; Holm, R. H. *Inorg. Chem.* **1998**, *37*, 328. (d) Naumov, N. G.; Virovets, A. V.; Sokolov, M. N.; Artemkina, S. B.; Fedorov, V. E. *Angew. Chem., Int. Ed. Engl.* **1998**, *37*, 1943. (e) Beauvais, L. G.; Shores, M. P.; Long, J. R. *Chem. Mater.* **1998**, *10*, 3783. (f) Shores, M. P.; Beauvais, L. G.; Long, J. R. *J. Am. Chem. Soc.* **1999**, *121*, 775. (g) Wang, R.; Zheng, Z. *J. Am. Chem. Soc.* **1999**, *121*, 3549. (h) Shores, M. P.; Beauvais, L. G.; Long, J. R. *Inorg. Chem.* **1999**, *38*, 1648. (i) Guilbaud, C.; Deluzet, A.; Domercq, B.; Molinié, P.; Coulon, C.; Boubekur, K.; Batail, P. *Chem. Commun.* **1999**, 1867. (j) Zheng, Z.; Gray, T. G.; Holm, R. H. *Inorg. Chem.* **1999**, *38*, 4888. (k) Yoshimura, T.; Umakoshi, K.; Sasaki, Y.; Sykes, A. G. *Inorg. Chem.* **1999**, *38*, 5557. (l) Gray, T. G.; Rudzinski, C. M.; Nocera, D. G.; Holm, R. H. *Inorg. Chem.* **1999**, *38*, 5932. (m) Kobayashi, N.; Ishizaka, S.; Yoshimura, T.; Kim, H.-B.; Sasaki, Y.; Kitamura, N. *Chem. Lett.* **2000**, 234. (n) Beauvais, L. G.; Shores, M. P.; Long, J. R. *J. Am. Chem. Soc.* **2000**, *122*, 2763. (o) Yoshimura, T.; Umakoshi, K.; Sasaki, Y.; Ishizaka, S.; Kim, H.-B.; Kitamura, N. *Inorg. Chem.* **2000**, *39*, 1765. (p) Bennett, M. V.; Shores, M. P.; Beauvais, L. G.; Long, J. R. *J. Am. Chem. Soc.* **2000**, *122*, 6664. (q) Chen, Z. N.; Yoshimura, T.; Abe, M.; Sasaki, Y.; Ishizaka, S.; Kim, H.-B.; Kitamura, N. *Angew. Chem., Int. Ed.* **2001**, *40*, 239. (r) Bennett, M. V.; Beauvais, L. G.; Shores, M. P.; Long, J. R. *J. Am. Chem. Soc.* **2001**, *123*, 8022. (s) Gabriel, J. C. P.; Boubekur, K.; Uriel, S.; Batail, P. *Chem. Rev.* **2001**, *101*, 2037.

(13) In contrast, efforts to place additional charge on the metal centers in a simple metal–anion framework by oxidation would change the electron count and therefore potentially alter the bonding preferences of the metal.

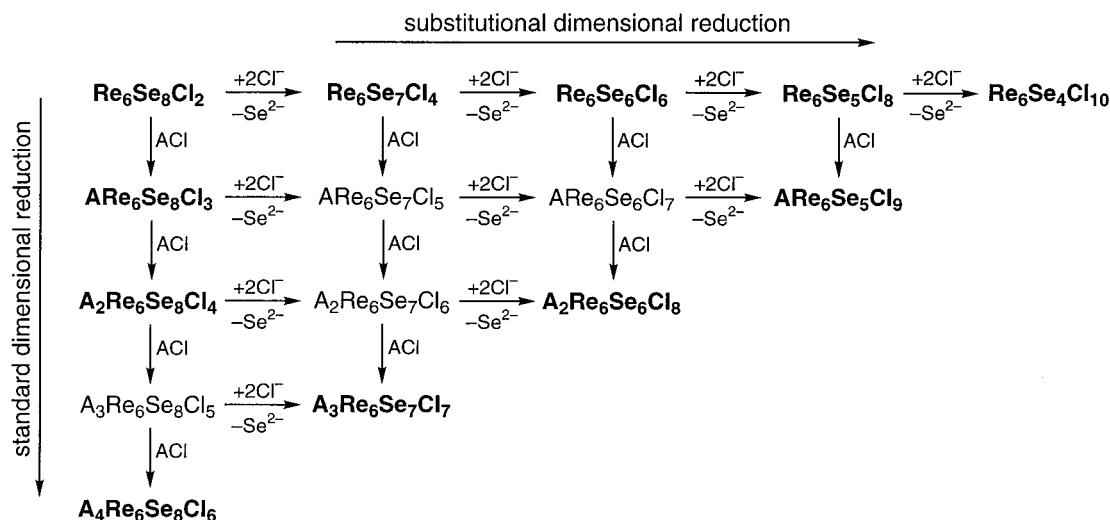
(14) (a) Leduc, L.; Perrin, A.; Sergent, M. C. *R. Acad. Sci., Ser. 2* **1983**, 296, 961. (b) Perrin, A.; Leduc, L.; Sergent, M. *Eur. J. Solid State Inorg. Chem.* **1991**, *28*, 919.

(15) Perrin, A.; Leduc, L.; Potel, M.; Sergent, M. *Mater. Res. Bull.* **1990**, *25*, 1227.

(16) (a) Ziebarth, R. P.; Corbett, J. D. *J. Am. Chem. Soc.* **1987**, *109*, 4844. (b) Ziebarth, R. P.; Corbett, J. D. *J. Am. Chem. Soc.* **1988**, *110*, 1132. (c) Ziebarth, R. P.; Corbett, J. D. *J. Solid State Chem.* **1989**, *80*, 56.

(17) (a) Perrin, A.; Sergent, M.; Fischer, Ø. *Mater. Res. Bull.* **1978**, *13*, 259. (b) Perrin, A.; Chevrel, R.; Sergent, M.; Fischer, Ø. *J. Solid State Chem.* **1980**, *33*, 43. (c) Hönle, W.; Flack, H. D.; Yvon, K. *J. Solid State Chem.* **1983**, *49*, 157. (d) Berry, F. J.; Gibbs, C. D. *J. Chem. Soc., Dalton Trans.* **1991**, 57. (e) Berry, F. J.; Gibbs, C. D.; Greaves, C. *J. Solid State Chem.* **1991**, *92*, 148.

(18) Neuhausen, J.; Finckh, E. W.; Tremel, W. *Inorg. Chem.* **1996**, *35*, 5622.

Scheme 1^a

^a Examples of compounds listed in bold face have been synthesized and structurally characterized;^{5,10,14,15} note that all formulas maintain a count of 24 metal-based valence electrons.

substitutions might reasonably be expected to alter the cluster charge. Indeed, an example of this behavior is evident in the recent report of Cs₃Re₅OsS₁₁,¹⁹ a 24-electron compound that is related to Li₄Re₆S₁₁²⁰ by substitution of Os^{IV} for A^IRe^{III}. Thus, Re₆Se₈Cl₂, which has served as the prototypical parent framework for dimensional reduction by standard methods⁵ and by core anion substitution,¹⁴ also presents a suitable candidate for investigating the possibility of carrying out dimensional reduction via heterometal substitution. Herein, we demonstrate the efficacy of this proposed technique with the synthesis of Re_{6-n}Os_nSe₈ cluster-containing solids, a number of which are soluble and supply new molecular cluster species.

Experimental Section

Preparation of Compounds. The compound [Re₆Se₈(PEt₃)₆]₂ was prepared as described previously.^{12a} Methanol and ethanol were distilled over Mg(OR)₂ (R = Me or Et) immediately prior to use, and water was distilled and deionized with a Milli-Q filtering system. Where noted, acetonitrile was distilled over CaH₂ prior to use. Fused silica ampules (with dimensions i.d. × o.d. × l = 9 × 11 × 85 mm), KCl (Fisher, 99.9%), and CsCl (Baker, 99.9%) were dried for 2 days at 150 °C prior to use. Other reagents, including Os (Strem, 99.8%, 100–200 mesh), Re (Cerac, 99.99%, –325 mesh), Se (Alfa, 99.999%, –325 mesh), and ReCl₅ (Cerac, 99.9%, –40 mesh), were used as purchased. Reactants were loaded under a pure dinitrogen atmosphere. High-temperature reactions were carried out in tube furnaces equipped with programmable controllers; temperatures were measured near the reactants and were typically ramped up at a rate of 3 °C/min. Loaded reaction ampules were situated with the reactants at the cooler end of the furnace and were elevated to a minimum incline of 30°. This was accomplished either by resting the warmer end of the tube on a piece of Fibrefrax within a horizontal tube furnace or by suspending the tube in a vertical tube furnace (with the lower end of the furnace open to air to ensure that the reactant end of the tube remained relatively cool). Product purity was checked by comparing the X-ray powder diffraction pattern of a bulk sample with one simulated from the single-crystal data.

Re₄Os₂Se₈Cl₄ (1). A mixture of Re (0.0377 g, 0.202 mmol), Os (0.192 g, 1.01 mmol), Se (0.160 g, 2.02 mmol), and ReCl₅ (0.110 g,

0.303 mmol) was intimately ground and transferred to a fused silica ampule, which was then cooled with liquid nitrogen, evacuated, and sealed. The ampule was heated at 850 °C for 4 days, cooled at 0.2 °C/min to 500 °C, and air-quenched. The product formed as shiny black platelike crystals embedded in a gray-black powder (for which all peaks in the X-ray powder diffraction pattern corresponded to OsSe₂). The crystals were separated from the powder by placing the mixture in diethyl ether and sonicating for 2 min; the powder rapidly dispersed into the ether and could be poured off as a slurry, leaving the crystals behind. Repeating this process three times afforded 0.0834 g (35%) of pure crystalline product. Electron microprobe analysis (EMA): Re_{4.09(4)}Os_{1.91(4)}Se_{7.99(8)}Cl_{4.48(8)}.

Cs₃Re₅OsSe₈Cl₆ (2). A mixture of Re (0.520 g, 2.79 mmol), Os (0.121 g, 0.635 mmol), Se (0.401 g, 5.08 mmol), ReCl₅ (0.138 g, 0.381 mmol), and CsCl (750 mg, 4.5 mmol) was intimately ground and transferred to a fused silica ampule, which was then cooled with liquid nitrogen, evacuated, and sealed. The ampule was heated at 875 °C for 4 days, cooled at 0.2 °C/min to 500 °C, and air-quenched. The resulting red-black solid was pulverized and then stirred in 75 mL of water for 30 min. Centrifugation followed by decantation yielded a deep red solution. The residual brown-black powder was stirred in an additional 40 mL of water to extract any remaining product into solution, which was again collected by centrifugation. The combined solutions were evaporated to dryness by heating at 70 °C to yield large red platelike crystals and a fine white powder. This solid was stirred under two successive 40 mL aliquots of ethanol for 15 min each and then washed with successive 10 mL aliquots of methanol and ether, dried in air, and collected to yield 1.10 g (73%) of product. Recrystallization by slow evaporation of an aqueous solution afforded dark wine-red crystals of Cs₃Re₅OsSe₈Cl₆·2H₂O suitable for X-ray analysis. ES⁻ MS (MeCN/H₂O): *m/z* 1048.395 ([Cs₃[Re₅OsSe₈Cl₆]²⁻), 983.941 ([Re₅OsSe₈Cl₆]²⁻). EMA: Cs_{2.63(15)}Re_{5.02(3)}Os_{0.98(3)}Se_{8.21(7)}Cl_{6.13(5)}.

Cs₂Re₄Os₂Se₈Cl₆ (3). A mixture of Re (0.267 g, 1.43 mmol), Os (0.170 g, 0.895 mmol), Se (0.283 g, 3.58 mmol), ReCl₅ (0.130 g, 0.358 mmol), and CsCl (0.157 g, 0.932 mmol) was intimately ground and transferred to a fused silica ampule, which was then cooled with liquid nitrogen, evacuated, and sealed. The ampule was heated at 875 °C for 4 days, cooled at 0.3 °C/min to 700 °C, soaked for 1 day, and then cooled at 0.3 °C/min to 500 °C and air-quenched. The resulting red-black solid was pulverized and then stirred in 50 mL of water for 30 min. Centrifugation followed by decantation separated an orange supernatant solution from a red-black powder. The solid was washed with two additional 50 mL aliquots of water, collected by centrifugation, and stirred under 200 mL of acetone for 2 h. The mixture was centrifuged, and the deep red solution was decanted. The residual

(19) Bronger, W.; Koppe, C.; Loevenich, M.; Schmitz, D.; Schuster, T. Z. *Anorg. Allg. Chem.* **1997**, 623, 695.

(20) (a) Bronger, W.; Miessen, H.-J. *J. Less-Common Met.* **1982**, 83, 29. (b) Bronger, W.; Miessen, H.-J.; Schmitz, D. *J. Less-Common Met.* **1983**, 95, 275. (c) Bronger, W.; Miessen, H.-J.; Müller, P.; Neugröschel, R. *J. Less-Common Met.* **1985**, 105, 303.

Table 1. Crystallographic Data^a for Re₄Os₂Se₈Cl₄ (**1**), Cs₃Re₅OsSe₈Cl₆·2H₂O (**2**·2H₂O), Cs₂Re₄Os₂Se₈Cl₆ (**3**), and K₂[Re₃Os₃Se₈Cl₆][Re₄Os₂Se₇Cl₇] (**4**)

	1	2 ·2H ₂ O	3	4
formula	Cl ₄ Os ₂ Re ₄ Se ₈	H ₄ Cl ₆ Cs ₃ O ₂ OsRe ₅ Se ₈	Cl ₆ Cs ₂ Os ₂ Re ₄ Se ₈	Cl ₁₃ K ₂ Os ₅ Re ₇ Se ₁₅
fw	1898.68	2400.34	2235.40	3978.08
T, K	155	161	153	160
space group	<i>P</i> 1	<i>P</i> 2 ₁ / <i>n</i>	<i>P</i> 3 ₁ <i>c</i>	<i>P</i> <i>n</i> 3̄
Z	2	2	2	2
a, Å	8.7946(7)	9.7255(7)	9.8333(2)	12.9553(3)
b, Å	8.8305(7)	12.8958(9)		
c, Å	11.9783(3)	11.8300(9)	14.12520(10)	
α, deg	87.8180(10)			
β, deg	84.896(3)	113.9180(10)		
γ, deg	63.824(4)			
V, Å ³	831.53(10)	1356.3(2)	1182.83(4)	2174.42(9)
d _{calc} , g/cm ³	7.583	5.878	6.276	6.076
R ₁ (wR ₂), ^b %	4.58 (9.51)	5.89 (16.06)	5.92 (14.57)	2.24 (3.09)

^a Obtained with graphite-monochromated Mo Kα (λ = 0.710 73 Å) radiation. ^b R₁ = Σ||F_o| - |F_c||/Σ|F_o|; wR₂ = {Σ[w(F_o² - F_c²)²]/Σ[w(F_o²)]^{1/2}.

brown-black powder was stirred in an additional 50 mL of acetone to extract any remaining product into solution, which was again collected by centrifugation. The combined acetone solutions were then evaporated to dryness to yield 0.720 g (72%) of product. ES⁻ MS (MeCN/DMF): *m/z* 2103.818 ([Cs[Re₄Os₂Se₈Cl₆]]⁻), 985.447 ([Re₄Os₂Se₈Cl₆]²⁻). EMA: Cs_{1.91(10)}Re_{4.09(3)}Os_{1.91(3)}Se_{8.02(8)}Cl_{6.56(9)}.

K₂[Re₃Os₃Se₈Cl₆][Re₄Os₂Se₇Cl₇] (4**).** A mixture of Re (0.0925 g, 0.497 mmol), Os (0.189 g, 0.994 mmol), Se (0.196 g, 2.48 mmol), ReCl₅ (0.0903 g, 0.248 mmol), and KCl (0.0185 g, 0.248 mmol) was intimately ground and transferred to a fused silica ampule, which was then cooled with liquid nitrogen, evacuated, and sealed. The ampule was heated at 875 °C for 5 days, cooled at 0.2 °C/min to 500 °C, and air-quenched. The resulting brown-black powder was pulverized and stirred in 75 mL of water for 45 min. Centrifugation followed by decantation separated a pale yellow supernatant solution from a brown powder. The solid was washed with an additional 50 mL aliquot of water, collected by centrifugation, and stirred under 250 mL of acetone for 12 h. The mixture was centrifuged, and the red solution was decanted. The residual brown-black powder was stirred in an additional 100 mL of acetone to extract any remaining product into solution, which was again collected by centrifugation. The combined acetone solutions were then reduced to dryness to yield 0.330 g (65%) of product. ES⁻ MS (MeCN/DMF): *m/z* 1973.904 ([Re₃Os₃Se₈Cl₆]⁻), 1927.948 ([Re₄Os₂Se₇Cl₇]⁻). EMA: K_{0.89(2)}Re_{3.58(8)}Os_{2.42(8)}Se_{7.41(11)}Cl_{7.08(14)}.

(Bu₄N)₃[Re₅OsSe₈Cl₆] (5**).** An excess amount of Bu₄NCl (0.5 g, 2 mmol) was added to a solution of **2** (0.500 g, 0.211 mmol) in 75 mL of water, causing immediate formation of a yellow-brown precipitate. The solid was collected by filtration, washed with 30 mL of water, and then dissolved in a minimum amount of acetonitrile. Recrystallization by ether vapor diffusion afforded large red rod-shaped crystals of (Bu₄N)₃[Re₅OsSe₈Cl₆]·2Et₂O, which were dried in air and collected to yield 0.558 g (98%) of product. Absorption spectrum (MeCN): λ_{max} (ε_M) 194 (461 700), 211 (sh, 284 300), 229 (sh, 130 900), 256 (94 350), 273 (sh, 65 940), 322 (sh, 17 410), 361 (sh, 7414), 405 (sh, 3911), 501 (sh, 496), 561 (sh, 175) nm. ES⁻ MS (MeCN): *m/z* 1104.942 ({(Bu₄N)[Re₅OsSe₈Cl₆]}²⁻), 655.961 ([Re₅OsSe₈Cl₆]³⁻). Anal. Calcd for C₄₈H₁₀₈Cl₆N₃Se₈Re₅Os: C, 21.41; H, 4.04; N, 1.56. Found: C, 21.53; H, 3.92; N, 1.70.

(Bu₄N)₂[Re₄Os₂Se₈Cl₆] (6**).** An excess amount of Bu₄NCl (0.2 g, 0.7 mmol) was added to a solution of **3** (0.216 g, 0.0970 mmol) in 30 mL of distilled acetonitrile, causing immediate formation of a white precipitate. The mixture was stirred for 5 min and filtered to afford a red-orange solution. Addition of 100 mL of ether precipitated an orange powder, which was collected by filtration. The solid was washed with successive 10 mL aliquots of water, 2-propanol, and ether and then dissolved in a minimum amount of acetonitrile. Recrystallization by diffusion of ether into the acetonitrile solution yielded 0.223 g (94%) of red crystalline product. Absorption spectrum (MeCN): λ_{max} (ε_M) 255 (28 760), 276 (sh, 22 150), 291 (sh, 16 140), 313 (sh, 11 170), 385 (sh, 4054), 462 (sh, 1051) nm. ES⁻ MS (MeCN/DMF): *m/z* 985.445 ([Re₄Os₂Se₈Cl₆]²⁻). Anal. Calcd for C₃₂H₇₂Cl₆N₂O₂Se₈Re₄Os: C, 16.58; H, 3.49; N, 1.07. Found: C, 16.68; H, 3.26; N, 1.18.

[Re₅OsSe₈(PEt₃)₆]Cl₃ (7**).** A solution of **5** (0.026 g, 0.0097 mmol) in 2 mL of DMF was sparged with dinitrogen for 30 min. After addition of PEt₃ (35 μL, 0.24 mmol), the reaction was heated at reflux for 60 h under dinitrogen. The reaction mixture was cooled; addition of 75 mL of ether precipitated a brown powder, which was collected by filtration. The solid was washed with two 50 mL aliquots of ether and dried in air. Recrystallization by diffusion of ether into an acetonitrile solution yielded 0.024 g (92%) of red crystals of [Re₅OsSe₈(PEt₃)₆]Cl₃·3CH₃CN. Absorption spectrum (MeCN): λ_{max} (ε_M) 283 (sh, 16 380), 347 (sh, 4660), 445 (sh, 967) nm. ES⁺ MS (MeCN): *m/z* 2532.597 ({[Re₅OsSe₈(PEt₃)₆]Cl₃}⁺), 1248.798 ({[Re₅OsSe₈(PEt₃)₆]Cl₂}⁺), 820.876 ([Re₅OsSe₈(PEt₃)₆]³⁺). ³¹P NMR (CD₃CN): δ (ppm) -17.4 (Os), -21.7 (4Re), -26.5 (Re). Anal. Calcd for C₃₆H₉₀Cl₃P₆Se₈Re₅Os: C, 16.84; H, 3.54; N, 0. Found: C, 16.63; H, 3.55; N, <0.2.

[Re₄Os₂Se₈(PEt₃)₆](I₃)₄ (8**).** A solution of **6** (0.026 g, 0.011 mmol) in 3 mL of DMF was sparged with dinitrogen for 45 min. After addition of PEt₃ (200 μL, 1.4 mmol), the reaction was heated at reflux for 6 days under dinitrogen. The reaction mixture was cooled; addition of 100 mL of ether precipitated a brown powder, which was collected by filtration. The solid was washed with two 50 mL aliquots of ether and dried in air. Recrystallization by diffusion of ether into an acetonitrile solution yielded red crystals of [Re₄Os₂Se₈(PEt₃)₆]Cl₄·4CH₃CN. Dissolution in DMF and gradual addition of I₂ resulted in formation of red-black crystals, which were collected by filtration, washed with 10 mL of ether, and dried in air to give 0.037 g (87%) of product. Absorption spectrum ((CD₃)₂SO): λ_{max} (ε_M) 296 (197 700), 366 (101 400) nm. ³¹P NMR (DMSO): trans, δ (ppm) -10.2 (2Os), -11.0 (4Re); cis δ (ppm) -5.1, -10.8, -14.9. Anal. Calcd for C₃₆H₉₀I₂P₆Se₈Re₄Os₂: C, 10.84; H, 2.28; N, 0. Found: C, 11.72; H, 2.40; N, <0.2.

trans,trans-[Re₄Os₂Se₈(PEt₃)₂Cl₄] (9**).** A solution of **6** (0.026 g, 0.011 mmol) in 2 mL of distilled acetonitrile was sparged with dinitrogen for 15 min. After addition of PEt₃ (7 μL, 0.04 mmol), the reaction was heated at reflux for 2 days under dinitrogen. The reaction mixture was cooled, and the solution was decanted. The maroon crystalline solid was washed with successive 10 mL aliquots of acetonitrile, water, 2-propanol, and ether, dried in air, and collected to yield 0.021 g (91%). The X-ray powder diffraction pattern of the solid collected indicated the presence of a small amount of an unidentified impurity.

X-ray Structure Determinations. Structures were determined for the seven compounds listed in Tables 1 and 2. Single crystals were coated with Paratone-N oil, attached to glass fibers, transferred to a Siemens SMART diffractometer, and cooled in a dinitrogen stream. Initial lattice parameters were obtained from a least-squares analysis of more than 30 centered reflections; these parameters were later refined against all data. A full hemisphere of data was collected for all compounds except **1**, for which a full sphere of data was collected. None of the crystals showed significant decay during data collection.

Table 2. Crystallographic Data^a for (Bu₄N)₃[Re₃OsSe₈Cl₆]·2Et₂O (**5**·2Et₂O), (Bu₄N)₂[Re₄Os₂Se₈Cl₆] (**6**), [Re₅OsSe₈(PEt₃)₆]Cl₃·3CH₃CN (**7**·3CH₃CN), [Re₄Os₂Se₈(PEt₃)₆]Cl₄·2CH₃CN (**8**·2CH₃CN), and trans-[Re₄Os₂Se₈(PEt₃)₂Cl₄] (**9**)

	5 ·2Et ₂ O	6	7 ·3CH ₃ CN	8 ·2CH ₃ CN	9
formula	C ₅₆ H ₁₂₈ Cl ₆ N ₃ O ₂ OsRe ₅ Se ₈	C ₃₂ H ₇₂ Cl ₆ N ₂ O ₂ Os ₂ Re ₄ Se ₈	C ₄₂ H ₉₀ Cl ₃ N ₃ OsP ₆ Re ₅ Se ₈	C ₄₀ H ₉₆ Cl ₄ N ₂ O ₂ P ₆ Re ₄ Se ₈	C ₁₂ H ₃₀ Cl ₄ Os ₂ P ₂ Re ₄ Se ₈
fw	2841.19	2454.50	2691.29	2689.69	2134.98
T, K	161	153	165	164	152
space group	<i>P</i> 1̄	<i>P</i> 2 ₁ / <i>c</i>	<i>C</i> 2/ <i>c</i>	<i>C</i> 2/ <i>c</i>	<i>P</i> 2 ₁ / <i>n</i>
Z	1	4	4	4	2
a, Å	12.5328(4)	22.4968(5)	15.7994(12)	15.8805(3)	9.2771(3)
b, Å	12.5489(5)	11.7187(3)	17.3613(13)	17.0904(2)	11.7511(4)
c, Å	13.9561(5)	22.3600(6)	24.979(2)	25.1555(3)	15.1970(5)
α, deg	85.7140(10)				
β, deg	76.9010(10)	112.4120(10)	97.0230(10)	96.7870(10)	103.884(2)
γ, deg	72.1220(10)				
V, Å ³	2034.54(13)	5449.6(2)	6800.4(9)	6779.5(2)	1608.31(9)
d _{calc} , g/cm ³	2.319	2.992	2.629	2.635	4.409
R1 (<i>w</i> R ₂), ^b %	5.30 (12.40)	3.71 (5.93)	3.07 (5.33)	2.64 (4.78)	3.77 (8.61)

^a Obtained with graphite-monochromated Mo Kα (λ = 0.710 73 Å) radiation. ^b R₁ = Σ||F_o - |F_c||/Σ|F_o|; wR₂ = {Σ[w(F_o² - F_c²)²]/Σ[w(F_o²)²]}^{1/2}.

Data were integrated and corrected for Lorentz and polarization effects using SAINT and were corrected for absorption effects using SADABS 2.0.

Space group assignments were based on systematic absences, *E* statistics, and successful refinement of the structures. Structures were solved by direct methods with the aid of successive difference Fourier maps and were refined against all data using the SHELXTL 5.0 software package. Thermal parameters for all non-hydrogen atoms were refined anisotropically, except for the partially occupied sites associated with disordered C and N atoms in the structures of **5**·2Et₂O, **7**·3CH₃CN, and **8**·2CH₃CN, which were refined isotropically. Hydrogen atoms associated with solvate water molecules and disordered carbon atoms were not included in the structural refinements. All other hydrogen atoms were assigned to ideal positions and refined using a riding model with an isotropic thermal parameter 1.2 times that of the attached carbon atom (1.5 times for methyl hydrogens). The metal sites in each cluster were assigned a mixed occupancy of 5/6Re + 1/6Os for the structures of **2**, **5**·2Et₂O, and **7**·3CH₃CN and 2/3Re + 1/3Os for the structures of **1**, **3**, **6**, and **8**·2CH₃CN; in these cases, efforts to localize the metals on specific sites showed no consistent improvement in the structural refinement. In the structure of **4**, the fractional Cl occupancy on the Se sites was refined, and the Os occupancy on the metal sites was then fixed according to the needs of charge balance. The chemical composition corresponding to the occupancies obtained by this method was found to be in good agreement with the results of electron microprobe and mass spectral analyses, all of which indicate an idealized formula of K₂[Re₃Os₃Se₈Cl₆][Re₄Os₂Se₇Cl₇]. One Bu₄N⁺ ion in the structure of **5**·2Et₂O is severely disordered; electron density peaks were assigned to partial carbon atom occupancies, and the overall shape, position, and size of this group of peaks was consistent with the presence of a disordered Bu₄N⁺ ion. Acetonitrile solvate molecules are disordered with Cl⁻ anions in the structures of **7**·3CH₃CN and **8**·2CH₃CN. These sites were modeled as half-occupied Cl atoms and half-occupied acetonitrile molecules, with one atom of the latter masked by the former in each structure and not discernible crystallographically.

Electrochemistry. Cyclic voltammograms were measured under a pure dinitrogen atmosphere with a Bioanalytical systems CV-50W voltammograph, using a platinum disk working electrode, a platinum wire auxiliary electrode, and a Ag/AgNO₃ reference electrode. Measurements were carried out in acetonitrile at concentrations of 0.001 M sample with 0.10 M Bu₄NPF₆ as a supporting electrolyte, except with measurements of **6**, for which the common ion effect required a 0.010 M solution of Bu₄NPF₆. Potentials were further calibrated by comparison with a (C₅H₅)₂Fe internal standard.

Electron Microprobe Analyses. Electron microprobe measurements were performed using a Cameca SX-51 electron microprobe equipped with five vertical high-resolution wavelength dispersive spectrometers. Results for cesium analyses were consistently low by ca. 10%, but this error was reduced significantly by measuring and correcting for cesium migration out of the electron beam. Chlorine analyses were systematically high; similar corrections failed to account for this error, but the

uniform discrepancy across samples suggests that some comparable, unidentified systematic effect is responsible.

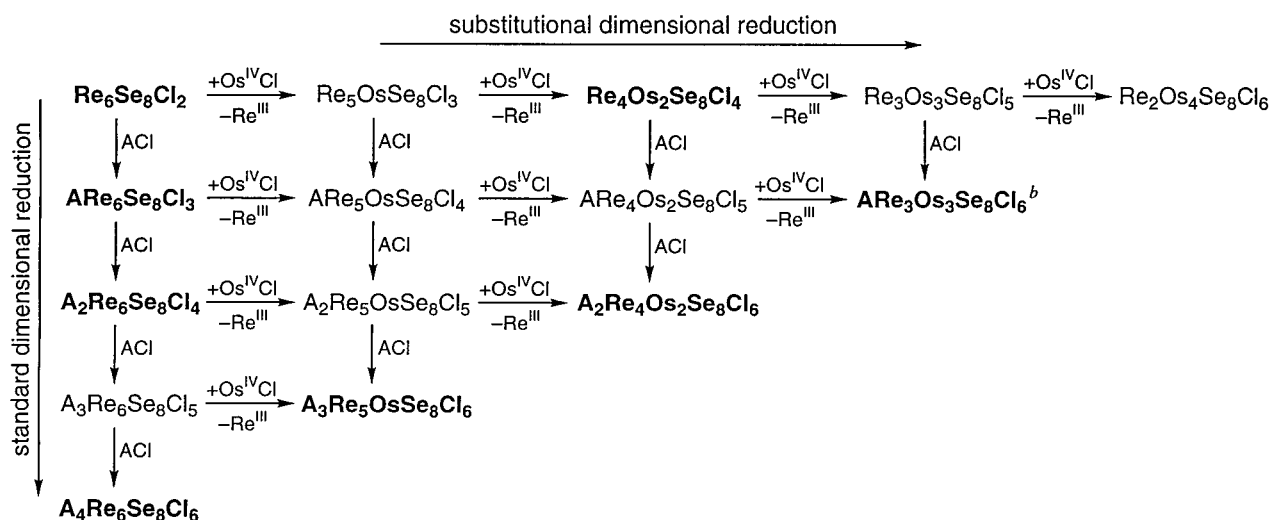
Other Physical Measurements. Absorption spectra were measured with a Hewlett-Packard 8453 spectrophotometer. Mass spectrometric measurements were performed on a Bruker Apex II 7 T actively shielded Fourier transform ion cyclotron resonance (FT-ICR) mass spectrometer equipped with an analytical electrospray ion source instrument. ³¹P{¹H} NMR spectra were measured with a Bruker DRX-500 MHz instrument; chemical shifts were referenced to an external sample of 85% H₃PO₄ (with negative values upfield). X-ray powder diffraction data were collected using Cu Kα (λ = 1.5406 Å) radiation on a Siemens D5000 diffractometer.

Electronic Structure Calculations. Density functional theory (DFT) calculations were performed using the Gaussian 98 quantum chemistry software package.²¹ Geometries were taken from crystal structures and idealized to the maximal point group symmetry of the clusters. Single-point energies were calculated using B3LYP functionals²² and the LANL2DZ effective core potentials (which included relativistic effects for all atoms except Cl) with the corresponding Gaussian basis sets.²³ To address the negative charge of the clusters, the basis set was augmented with diffuse orbitals derived from the highest angular momentum orbitals used for each atom by multiplying the lowest exponent by 0.4. Polarization functions were also included; d polarization functions for Cl and Se were taken from the 6-311G⁺ basis set, and f polarization functions for Re and Os were taken from a previous report.²⁴

Results and Discussion

Solid-State Syntheses. In general, solid-state syntheses were carried out in a manner consistent with previous preparations of rhenium chalcogenide cluster phases.^{5,10,14,15} Mixtures of

- (21) Frisch, M. J.; Trucks, G. W.; Schlegel, H. B.; Scuseria, G. E.; Robb, M. A.; Cheeseman, J. R.; Zakrzewski, V. G.; Montgomery, J. A.; Stratmann, R. E.; Burant, J. C.; Dapprich, S.; Millam, J. M.; Daniels, A. D.; Kudin, K. N.; Strain, M. C.; Farkas, O.; Tomasi, J.; Barone, V.; Cossi, M.; Cammi, R.; Mennucci, B.; Pomelli, C.; Adamo, C.; Clifford, S.; Ochterski, J.; Petersson, G. A.; Ayala, P. Y.; Cui, Q.; Morokuma, K.; Malick, D. K.; Rabuck, A. D.; Raghavachari, K.; Foresman, J. B.; Cioslowski, J.; Ortiz, J. V.; Stefanov, B. B.; Liu, G.; Liashenko, A.; Piskorz, P.; Komaromi, I.; Gomperts, R.; Martin, R. L.; Fox, D. J.; Keith, T.; Al-Laham, M. A.; Peng, C. Y.; Nanayakkara, A.; Gonzalez, C.; Challacombe, M.; Gill, P. M. W.; Johnson, B. G.; Chen, W.; Wong, M. W.; Andres, J. L.; Head-Gordon, M.; Replogle, E. S.; Pople, J. A. *Gaussian 98 (Revision A.7)*; Gaussian, Inc.: Pittsburgh, PA, 1998.
- (22) (a) Vosky, S. H.; Wilk, L.; Nusair, M. *Can. J. Phys.* **1980**, *58*, 1200. (b) Becke, A. D. *J. Chem. Phys.* **1993**, *98*, 5648. (c) Lee, C.; Yang, W.; Parr, R. G. *Phys. Rev. B* **1988**, *37*, 785.
- (23) (a) Hay, P. J.; Wadt, W. R. *J. Chem. Phys.* **1985**, *82*, 270. (b) Wadt, W. R.; Hay, P. J. *J. Chem. Phys.* **1985**, *82*, 284. (c) Hay, P. J.; Wadt, W. R. *J. Chem. Phys.* **1985**, *82*, 299. (d) Dunning, T. H., Jr.; Hay, P. J. In *Modern Theoretical Chemistry*; Schaefer, H. F., Ed.; Plenum: New York, 1976; Vol. 3, p 1.

Scheme 2^a

^a Examples of compounds listed in bold face have been synthesized and structurally characterized;^{5,10} note that all formulas maintain a count of 24 metal-based valence electrons. ^b Cocrystallized with KRe₄Os₂Se₇Cl₇ in compound 4.

elemental or binary reagents were intimately ground, sealed in evacuated fused silica tubes, and heated at approximately 850 °C. Slow cooling rates were employed to enhance crystal growth. A number of steps were also necessary to prevent the reactants from segregating within the reaction tube and ensure homogeneity of products. The thermal gradient across each tube was minimized to a temperature difference of less than 20 °C, and the reactants were situated at the cooler end of the tube to prevent migration of volatile components away from the reaction mixture. This is of particular importance for the reactions involving CsCl: tubes subjected to larger thermal gradients were found to give very low yields, with OsSe₂, Cs₂Re₆Se₈Cl₄,^{5a} Cs₂ReCl₆, and unreacted CsCl forming the major products. Additionally, the warmer end of each reaction tube was elevated at a minimum incline of 30° to restrict flow of molten components away from the reaction mixture.

Dimensional reduction of Re₆Se₈Cl₂ strictly via substitution of Os for Re provides the target compounds listed along the horizontal axis at the top of Scheme 2. Efforts to produce these compounds have thus far resulted in the synthesis of just Re₄Os₂Se₈Cl₄. Reactions targeting Re₅OsSe₈Cl₃, Re₄Os₂Se₈Cl₄, and Re₃Os₃Se₈Cl₅ through use of a stoichiometric mixture of reagents failed to give the desired products, as did reactions utilizing additional ReCl₅, Os, or OsSe₂.²⁵ In such attempts, the major products identified by X-ray powder diffraction were OsSe₂ and Re₆Se₈Cl₂; these were typically accompanied by an oily green-brown residue that condensed onto the walls of the tube upon cooling, decomposed quickly in air, and was assumed to consist of a selenium–chlorine compound. Only when excess osmium was supplied in reactions targeting a stoichiometry of Re₂Os₄Se₈Cl₆ was the heterometallic phase Re₄Os₂Se₈Cl₄ obtained in substantial quantity. The compound forms as black platelike crystals that can be separated from the other products by sonication in ether.

Applying standard dimensional reduction in conjunction with Os substitution opens up the entire grid of target compounds shown in Scheme 2, including several saturated phases contain-

ing discrete molecular clusters. Note that the choice of counteranion A is considered an experimental variable for such dimensional reduction reactions.¹ In this case, CsCl was initially selected as the dimensional reduction agent, owing to its prior success in dismantling Re₆Q₈Cl₂ (Q = S, Se).⁵ Indeed, utilizing CsCl, the new mixed-metal phases Cs₃Re₅OsSe₈Cl₆ and Cs₂Re₄Os₂Se₈Cl₆ are readily prepared. A mixture of the two compounds is generally obtained; however, it was found that the suspected equilibrium could be driven toward the former by supplying approximately 5 equiv of excess CsCl or toward the latter by using a stoichiometric mixture. The different solubility properties of the products enables their facile separation, and mass spectra of the resulting solutions confirm the presence of the clusters [Re₅OsSe₈Cl₆]³⁻ and [Re₄Os₂Se₈Cl₆]²⁻ (see Figure 2). No evidence for further incorporation of osmium to form [Re₃Os₃Se₈Cl₆]⁻ was observed in the products from reactions employing CsCl. Recognizing that a trisubstituted monoanionic cluster could be stabilized using potassium as a counteranion in the compound KRe₆Se₅Cl₉,¹⁵ KCl was tested as a dimensional reduction agent. Reactions targeting KRe₃Os₃Se₈Cl₆ did in fact afford crystals isostructural with KRe₆Se₅Cl₉, but mass spectrometry showed these to contain a mixture of clusters, including [Re₃Os₃Se₈Cl₆]⁻, [Re₄Os₂Se₇Cl₇]⁻, and [Re₅OsSe₆Cl₈]⁻. Using a slight excess OsSe₂²⁵ was found to increase the proportion of osmium-rich clusters, permitting isolation of K₂[Re₃Os₃Se₈Cl₆][Re₄Os₂Se₇Cl₇]. The separation of these two monoanionic clusters in solution is expected to be difficult and was not attempted, nor were other dimensional reduction agents enlisted in efforts to obtain a solid product containing exclusively [Re₃Os₃Se₈Cl₆]⁻.

Structures of Products of Dimensional Reduction. As indicated in Scheme 2, the compound Re₄Os₂Se₈Cl₄ is formally related to Re₆Se₈Cl₂ via incorporation of an additional 2 equiv of chloride anions with concomitant substitution of Os^{IV} for Re^{III}. X-ray analysis of a single crystal revealed the two-dimensional framework of interlinked cluster cores depicted in Figure 3. Although the dimensionality of the framework is no lower than in the Re₆Se₈Cl₂ parent, the additional chloride ligands serve to convert the rhombic Re₂Se₂ linkages into single intercluster bridges, thereby lowering its connectedness¹ from eight to four. Interestingly, the resulting structure is quite different from that of Re₆Se₆Cl₆,^{14b} which is isostructural with

(24) Ehlers, A. W.; Bohme, M.; Dapprich, S.; Gobbi, A.; Hollwarth, A.; Jonas, V.; Kohler, K. F.; Stegmann, R.; Veldkamp, A.; Frenking, G. *Chem. Phys. Lett.* **1993**, *208*, 111.

(25) Note that OsSe₂ was not employed as a reactant; instead, additional osmium and selenium were added to create target mixtures of composition Re₄Os₂Se₈Cl₄·xOsSe₂.

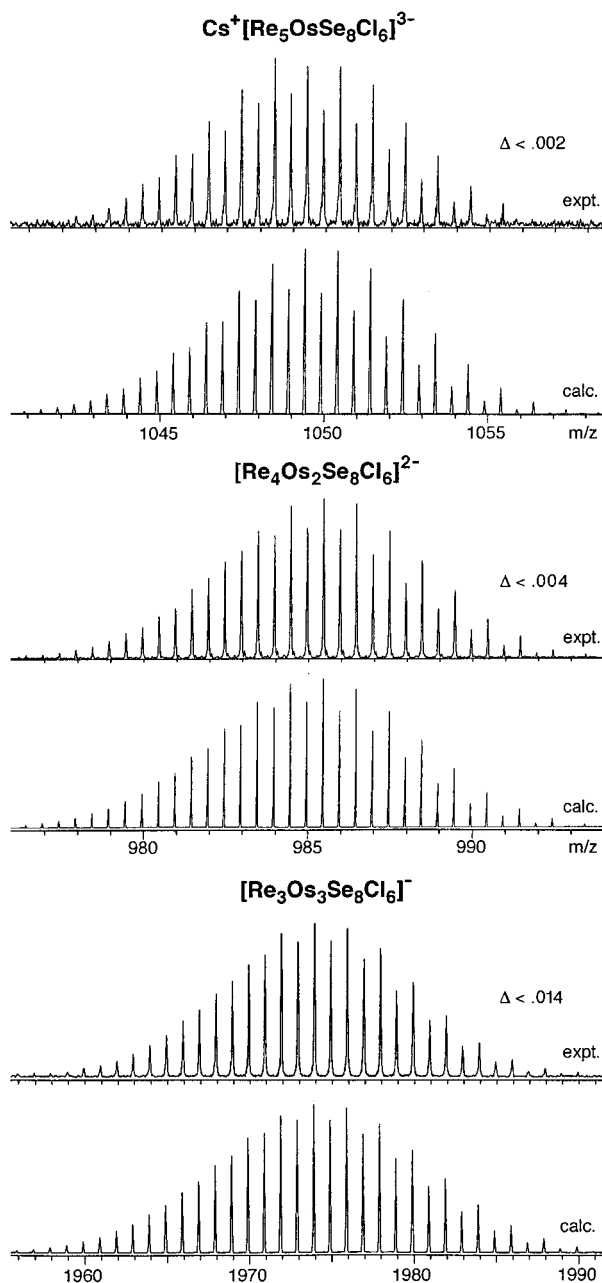


Figure 2. Parent ion peaks from the FT-ICR electrospray mass spectra obtained for solutions of $\text{Cs}_3\text{Re}_5\text{OsSe}_8\text{Cl}_6$, $\text{Cs}_2\text{Re}_4\text{Os}_2\text{Se}_8\text{Cl}_6$, and $\text{K}_2[\text{Re}_3\text{Os}_3\text{Se}_8\text{Cl}_6][\text{Re}_4\text{Os}_2\text{Se}_7\text{Cl}_7]$. In each case, the isotope distribution, intensities, and masses closely match the simulated data.

$\text{Mo}_6\text{Cl}_{12}$ (see Figure 1),⁷ and also features a four-connected, two-dimensional framework. Within a two-dimensional sheet of $\text{Re}_4\text{Os}_2\text{Se}_8\text{Cl}_4$, the connections between cluster cores are formed along one direction through shared outer chloride ligands (just as in $\text{Re}_6\text{Se}_6\text{Cl}_6$), while linkages along the other direction arise when a selenium atom from one cluster core serves as an apical ligand for the neighboring cluster. These unsupported M–Qⁱ bridges between clusters are to our knowledge without precedent in M_6Q_8 -type cluster chemistry. The framework is further differentiated by the presence of two distinct environments for the cluster cores, one with an outer ligand shell made up of two terminal chloride ligands, two bridging chloride ligands, and two selenium atoms from neighboring cluster cores ($=[\text{M}_6\text{Se}_i^i\text{Se}^{a-i/2}\text{Cl}_2\text{Cl}^{a-2/2}]$) and one providing the bridging selenium atoms and forming its apical ligand shell from four terminal and two bridging chloride ligands ($=[\text{M}_6\text{Se}_i^i\text{Se}^{i-2/2}]$ -

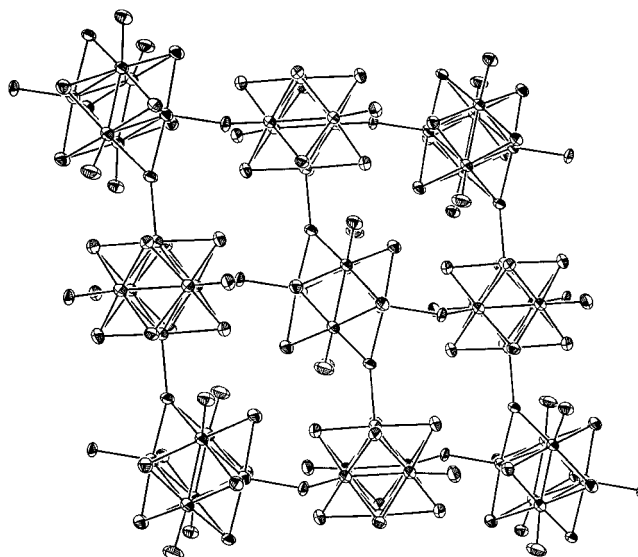


Figure 3. Portion of the structure of two-dimensional $\text{Re}_4\text{Os}_2\text{Se}_8\text{Cl}_4$. Ellipsoids are drawn at the 80% probability level. Each cluster core consists of six metal and eight selenium atoms; all other atoms are chlorine atoms. Crystallographic inversion centers are located at the center of each cluster and in the center of each four-cluster ring. The central cluster is apically ligated by two bridging and four terminal chloride ions, while its neighbors are ligated by two bridging and two terminal chloride ions and two bridging selenide ions.

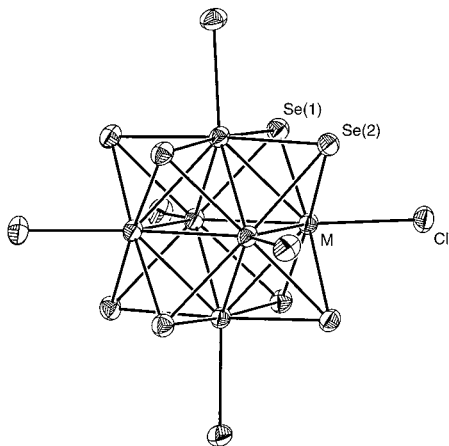
$\text{Cl}_4\text{Cl}^{a-2/2}$). This raises the possibility that neighboring clusters might actually possess two different core compositions, with the average corresponding to four rhenium and two osmium atoms. However, no crystallographic evidence could be found to support such a scenario, and low-temperature excision methods¹¹ have thus far proven unsuccessful in extricating the clusters from the framework.

The presence of metal sites with different coordination environments in the structure of $\text{Re}_4\text{Os}_2\text{Se}_8\text{Cl}_4$ suggests that the rhenium and osmium atoms could potentially be distributed in an ordered fashion. In particular, although it would account for only half of the osmium atoms, the novelty of the intercluster M–Se linkages might be taken to indicate that osmium is associated with these metal sites. For want of a better probe, X-ray crystallography was utilized in an attempt to identify any ordering of the osmium atoms within the framework. Care was taken to select only crystals of the utmost quality, and a full sphere of data was collected to improve the absorption correction and increase the statistical significance of minor changes in electron density near the heavy metal atoms. The metal–anion distances would be expected to vary from metal to metal in an ordered structure, since the additional charge of an Os^{IV} center should lead to shorter bond lengths as a result of the increased Coulombic interaction and improved energetic match of the metal and anion orbitals. This type of effect is borne out in the structure of $\text{Re}_6\text{Se}_6\text{Cl}_6$,^{14b} where, for example, the increased positive charge of the cluster core leads to slightly shorter terminal Re–Cl distances than observed¹⁰ in $\text{Re}_6\text{Se}_8\text{Cl}_2$ (see Table 3). While the mean metal–anion distances in $\text{Re}_4\text{Os}_2\text{Se}_8\text{Cl}_4$ are similar to those in $\text{Re}_6\text{Se}_6\text{Cl}_6$, comparing metal sites within the structure fails to reveal any of the disparities expected if the osmium atoms were localized. Furthermore, the results from structural refinements against several different crystallographic data sets, employing all possible ordered, partially ordered, and fully disordered models, offer no consistent variation in wR_2 .²⁶ Thus, despite the chemical nonequivalence

Table 3. Selected Mean Interatomic Distances (Å) and Angles (deg) for Re₆Se₈Cl₂,¹⁰ Re₄Os₂Se₈Cl₄ (**1**), and Re₆Se₆Cl₆^{14b a}

	Re ₆ Se ₈ Cl ₂	Re ₄ Os ₂ Se ₈ Cl ₄	Re ₆ Se ₆ Cl ₆
M—M	2.64(2)	2.633(11)	2.614(3)
M—Q	2.52(1)	2.515(11)	2.506(9)
M—μ ₄ -Se	2.62(1)	2.577(3)	
M—μ ₂ -Cl		2.444(7)	2.465(7)
M—Cl ^t	2.38(1)	2.356(8)	2.360(8)
M—Q—M	62.9(4)	63.2(3)	62.9(1)
Q—M—Q	90.2(3)	90.2(6)	89.9(3)
		175.9(4)	176.5(2)
Q—M—Cl	91.5(8)	92(3)	92(2)
M—μ ₄ -Se—M	81.7(1)	129.78(12)	
M—μ ₂ -Cl—M		125.5(3)	132.7(3)

^a M = Re or Os; Q = μ₃ core Se or Cl; t = terminal.

**Figure 4.** [Re₄Os₂Se₈Cl₆]²⁻ anion in the structure of **3**. Ellipsoids are drawn at the 50% probability level. The cluster has crystallographically imposed D₃ symmetry, with the 3-fold axis running through Se(1).

of certain metal sites, there is as yet no evidence that the metal atoms are ordered within the structure.

The crystal structures of molecular salts produced by combining heterometal substitution with standard dimensional reduction provide somewhat less ambiguous geometric information on the mixed-metal clusters. The compound Cs₂Re₄Os₂Se₈Cl₆ can be viewed as the result of dimensional reduction of Re₄Os₂Se₈Cl₄ with 2 equiv of CsCl. As expected for a saturated phase, its structure exhibits discrete [Re₄Os₂Se₈Cl₆]²⁻ clusters (see Figure 4). The interatomic distances and angles associated with the [Re₄Os₂Se₈]⁴⁺ cluster core (see Table 4) are comparable to those observed in Re₄Os₂Se₈Cl₄ (see Table 3). Since all of the cluster metal sites are crystallographically equivalent, the structure of Cs₂Re₄Os₂Se₈Cl₆ again reveals no ordering of the rhenium and osmium atoms. Although crystals of the parent compounds Re₅OsSe₈Cl₃ and Re₃Os₃Se₈Cl₅ could not be obtained, clusters with cores bearing the corresponding compositions are featured in the structures of Cs₃Re₅OsSe₈Cl₆ and K₂[Re₃Os₃Se₈Cl₆][Re₄Os₂Se₇Cl₇]. Both structures contain isolated clusters with the familiar face-capped octahedral geometry, and neither displays ordering of the rhenium and osmium atoms. Selected mean interatomic distances and angles for the new rhenium—osmium clusters are listed in Table 4, along with those of [Re₆Se₈Cl₆]⁴⁻.^{5a} In the comparison of metric parameters, the most noticeable trends are the steady decrease in terminal M—Cl distances, and, to a lesser extent, in M—Q distances, as the

charge on the cluster core increases from +2 in [Re₆Se₈Cl₆]⁴⁻ to +5 in [Re₃Os₃Se₈Cl₆]⁻ and [Re₄Os₂Se₇Cl₇]⁻.

Multiple isomers are possible for face-capped octahedral clusters obtained by substitution of more than one core atom. The disubstituted cluster [Re₄Os₂Se₈Cl₆]²⁻ (Figure 4) has two possible isomers: one in which the osmium atoms are located at trans vertexes of the M₆ octahedron and one in which they are located at cis vertexes. Similarly, *mer* and *fac* isomers are possible for the [Re₃Os₃Se₈Cl₆]⁻ cluster. Of course, in either case, it is impossible to establish the relative ratios of isomers crystallographically owing to disorder of the rhenium and osmium atoms. Substitution of both metal and anion sites in the core can lead to larger numbers of isomers. For example, four isomers are possible for the [Re₄Os₂Se₇Cl₇]⁻ clusters present in the structure of **4**: one involving a trans arrangement of osmium atoms and three involving a cis arrangement. The possible isomers for a face-capped octahedral [Re_{6-n}Os_nSe_{8-q}Cl_q]^{(2+n+q)+} (n + q = 0, 1, 2, 3, 4) cluster core, or indeed for any [M_{6-n}M'_nQ_{8-q}Q'_q] cluster adopting this geometry, are enumerated in Table 5.²⁷ Notice how, as the number of substitutions n + q and the charge of the cluster core increase, the number of possible compositions and isomers also increase. Conceivably, these factors play a role in the formation of a mixture of monoanionic clusters from reactions targeting KRe₃Os₃Se₈Cl₆.

Solution Chemistry. Consistent with the solubility properties of analogous salts containing [Re₆Q_{8-q}X_{6+q}]^{(4-q)-} (Q = S, Se; X = Cl, Br; q = 1–3) clusters,²⁸ Cs₃Re₅OsSe₈Cl₆ readily dissolves in water and acetonitrile, while Cs₂Re₄Os₂Se₈Cl₆ and K₂[Re₃Os₃Se₈Cl₆][Re₄Os₂Se₇Cl₇] are soluble in such polar organic solvents as acetonitrile and acetone. Since the rhenium and osmium atoms in these solids could not be differentiated by X-ray crystallography, additional proof of osmium incorporation into the clusters was sought. Indeed, a reasonable alternative explanation for the altered cluster charge might invoke oxidation, which is known to occur for clusters with the [Re₆Se₈]²⁺ core.^{12j,p,r} Solutions of the cluster-containing salts were therefore analyzed by FT-ICR mass spectrometry, producing data with a resolution of approximately 0.05 amu/q_e and an accuracy of ±0.003 amu/q_e. Since replacement of one rhenium atom with one osmium atom affords a mass increase of ca. 4 amu, the isotope distribution of an oxidized [Re₆Se₈Cl₆]³⁻ cluster would be significantly shifted from that of the [Re₅OsSe₈Cl₆]³⁻ cluster. As shown in Figure 2, the agreement of the experimental data with calculated masses and isotope distributions firmly establishes the presence of osmium in individual cluster molecules. Additionally, it is important to note that the mass spectra obtained are consistent with the chemical formulations assigned to the solids, ruling out any extensive compositional disorder in the crystal structures (beyond that already established for compound **4**).²⁹

Metathesis reactions carried out in solution readily produce (Bu₄N)₃[Re₅OsSe₈Cl₆] and (Bu₄N)₂[Re₄Os₂Se₈Cl₆], which are then soluble in a wider range of polar organic solvents. The crystal structures of these compounds feature the clusters in a state that is relatively unperturbed by interactions with the counteranions. Selected mean interatomic distances and angles

(26) Changes were observed on the order of 0.0001–0.0003; to test the statistical significance of these variations, the process was repeated on three data sets of comparable quality. Each exhibited fluctuations of a similar magnitude, but the apparent preferred sites for osmium localization varied across data sets.

(27) Structures of the different isomers have been deposited as Supporting Information.

(28) (a) Uriel, S.; Boubekeur, K.; Gabriel, J.-C.; Batail, P.; Orduna, J. *Bull. Soc. Chim. Fr.* **1996**, 133, 783. (b) Guilbaud, C.; Gabriel, J.-C.; Boubekeur, K.; Batail, P. *C. R. Acad. Sci., Ser. C* **1998**, 1, 627. (c) Slougui, A.; Perrin, A.; Sergent, M. *J. Solid State Chem.* **1999**, 147, 358. (d) Yarovoi, S. S.; Mironov, Y. V.; Solodovnikov, S. F.; Virovets, A. V.; Fedorov, V. E. *Mater. Res. Bull.* **1999**, 34, 1345.

Table 4. Selected Mean Interatomic Distances (Å) and Angles (deg) for the Clusters in $\text{Ti}_3\text{Re}_6\text{Se}_8\text{Cl}_7$,^{5a} $\text{Cs}_3\text{Re}_5\text{OsSe}_8\text{Cl}_6 \cdot 2\text{H}_2\text{O}$ ($2 \cdot 2\text{H}_2\text{O}$), $\text{Cs}_2\text{Re}_4\text{Os}_2\text{Se}_8\text{Cl}_6$ (**3**), and $\text{K}_2[\text{Re}_3\text{Os}_3\text{Se}_8\text{Cl}_6][\text{Re}_4\text{Os}_2\text{Se}_7\text{Cl}_7]$ (**4**)^a

	$[\text{Re}_6\text{Se}_8\text{Cl}_6]^{4-}$	$[\text{Re}_5\text{OsSe}_8\text{Cl}_6]^{3-}$	$[\text{Re}_4\text{Os}_2\text{Se}_8\text{Cl}_6]^{2-}$	$[\text{Re}_{3.5}\text{Os}_{2.5}\text{Se}_{7.5}\text{Cl}_{6.5}]^{1-b}$
M–M	2.614(5)	2.624(5)	2.623(8)	2.618(2)
M–Q	2.523(3)	2.518(8)	2.509(10)	2.502(9)
M–Cl ^t	2.431(8)	2.418(15)	2.402(4)	2.379
M–Q–M	62.4(1)	62.8(2)	63.0(3)	63.1(2)
M–M–Cl ^t	135(1)	135(2)	135(2)	135.0(9)
Q–M–Q	90.0(1)	90.0(6)	89.9(12)	90.0(4)
	176.7(1)	176.5(5)	176.1(6)	176.2(6)
Q–M–Cl ^t	91(1)	91.7(15)	91.9(14)	91.9(10)

^a M = Re or Os; Q = core Se or Cl; t = terminal. ^b Average values for the 1:1 mixture of $[\text{Re}_3\text{Os}_3\text{Se}_8\text{Cl}_6]^-$ and $[\text{Re}_4\text{Os}_2\text{Se}_7\text{Cl}_7]^-$ clusters cocrystallized in **4**.

Table 5. Number of Possible Isomers for Face-Capped Octahedral Cluster Cores of Composition $[\text{Re}_{6-n}\text{Os}_n\text{Se}_{8-q}\text{Cl}_q]^{(2+n+q)+}$ ($n + q = 0-4$)^a

q	n				
	0	1	2	3	4
0	$[\text{Re}_6\text{Se}_8]^{2+}$, 1	$[\text{Re}_5\text{OsSe}_8]^{3+}$, 1	$[\text{Re}_4\text{Os}_2\text{Se}_8]^{4+}$, 2	$[\text{Re}_3\text{Os}_3\text{Se}_8]^{5+}$, 2	$[\text{Re}_2\text{Os}_4\text{Se}_8]^{6+}$, 2
1	$[\text{Re}_6\text{Se}_7\text{Cl}]^{3+}$, 1	$[\text{Re}_5\text{OsSe}_7\text{Cl}]^{4+}$, 2	$[\text{Re}_4\text{Os}_2\text{Se}_7\text{Cl}]^{5+}$, 4	$[\text{Re}_3\text{Os}_3\text{Se}_7\text{Cl}]^{6+}$, 6	
2	$[\text{Re}_6\text{Se}_6\text{Cl}_2]^{4+}$, 3	$[\text{Re}_5\text{OsSe}_6\text{Cl}_2]^{5+}$, 7	$[\text{Re}_4\text{Os}_2\text{Se}_6\text{Cl}_2]^{6+}$, 16		
3	$[\text{Re}_6\text{Se}_5\text{Cl}_3]^{5+}$, 3	$[\text{Re}_5\text{OsSe}_5\text{Cl}_3]^{6+}$, 10			
4	$[\text{Re}_6\text{Se}_4\text{Cl}_4]^{6+}$, 6				

^a Pairs of enantiomers were counted as just one isomer.

Table 6. Selected Mean Interatomic Distances (Å) and Angles (deg) for the Clusters in $(\text{Bu}_4\text{N})_3[\text{Re}_5\text{OsSe}_8\text{Cl}_6] \cdot 2\text{Et}_2\text{O}$ (**5**· $2\text{Et}_2\text{O}$), $(\text{Bu}_4\text{N})_3[\text{Re}_6\text{Se}_7\text{Cl}_7] \cdot 2\text{Et}_2\text{O}$,³⁰ $(\text{Bu}_4\text{N})_2[\text{Re}_4\text{Os}_2\text{Se}_8\text{Cl}_6]$ (**6**), and $(\text{Pr}_4\text{N})_2[\text{Re}_6\text{Se}_6\text{Cl}_8]^{31 a}$

	$[\text{Re}_5\text{OsSe}_8\text{Cl}_6]^{3-}$	$[\text{Re}_6\text{Se}_7\text{Cl}_7]^{3-}$	$[\text{Re}_4\text{Os}_2\text{Se}_8\text{Cl}_6]^{2-}$	$[\text{Re}_6\text{Se}_6\text{Cl}_8]^{2-}$
M–M	2.624(5)	2.623(2)	2.625(3)	2.613(4)
M–Q	2.514(4)	2.512(5)	2.507(6)	2.505(2)
M–Cl ^t	2.426(1)	2.428(7)	2.400(7)	2.380(3)
M–Q–M	62.9(1)	63.0(1)	63.2(2)	63.2(2)
M–M–Cl ^t	135.0(6)	134.9(7)	135.0(11)	135(2)
Q–M–Q	89.9(3)	89.9(3)	89.9(3)	
	176.4(4)	176.3(3)	176.1(3)	
Q–M–Cl ^t	91.8(6)	91.8(7)	91.9(11)	91.9(2)

^a M = Re or Os; Q = core Se or Cl; t = terminal.

within the clusters are listed in Table 6, along with those of $[\text{Re}_6\text{Se}_7\text{Cl}_7]^{3-}$ and $[\text{Re}_6\text{Se}_6\text{Cl}_8]^{2-}$ for comparison.^{30,31} Interestingly, while the trianionic species $[\text{Re}_5\text{OsSe}_8\text{Cl}_6]^{3-}$ and $[\text{Re}_6\text{Se}_7\text{Cl}_7]^{3-}$ are essentially congruent, minor differences in M–M and M–Cl distances are apparent between $[\text{Re}_4\text{Os}_2\text{Se}_8\text{Cl}_6]^{2-}$ and $[\text{Re}_6\text{Se}_6\text{Cl}_8]^{2-}$. Despite the similarities in geometry and charge, these two types of core substituted clusters are distinguished by a fundamental difference in reactivity: core halide anions are susceptible to facile exchange for more negatively charged ligands (such as oxide),^{31,32} whereas core selenide anions are not. Note that this difference in reactivity suggests a possible means of separating $[\text{Re}_4\text{Os}_2\text{Se}_7\text{Cl}_7]^-$ from $[\text{Re}_3\text{Os}_3\text{Se}_8\text{Cl}_6]^-$ by changing the solubility properties of the former cluster via substitution of its inner chloride ligand.

Substitution of the outer chloride ligands of $[\text{Re}_5\text{OsSe}_8\text{Cl}_6]^{3-}$ and $[\text{Re}_4\text{Os}_2\text{Se}_8\text{Cl}_6]^{2-}$ is accomplished by heating the clusters with PET_3 in DMF. In the latter case, somewhat more forcing conditions are required to achieve complete substitution (see Figure 5), possibly as a consequence of the stronger attraction between the anionic Cl^- ligands and the more highly charged cluster core. As evident from inspection of Table 7, the resulting clusters $[\text{Re}_5\text{OsSe}_8(\text{PET}_3)_6]^{3+}$ and $[\text{Re}_4\text{Os}_2\text{Se}_8(\text{PET}_3)_6]^{4+}$ are remarkably similar in geometry and furthermore display little deviation from the structure of $[\text{Re}_6\text{Se}_8(\text{PET}_3)_6]^{2+}$.^{12a} The most noteworthy change in the cluster cores upon replacing the anionic chloride ligands with neutral PET_3 ligands is a slight expansion of the central M_6 octahedron, which is reflected in the increase in M–M distances and M–Se–M angles (see Tables 6 and 7). As observed for analogous reactions between PET_3 and the clusters $[\text{Re}_6\text{Se}_8\text{I}_6]^{4-}$ and $[\text{Re}_6\text{S}_8\text{Br}_6]^{4-}$,^{12a,c} the use of less forcing conditions permits the isolation of partially substituted species. Here, however, the ligand exchange appears to be influenced by the different metal sites, leading to the synthesis of a diphosphine cluster $\text{trans,trans-}[\text{Re}_4\text{Os}_2\text{Se}_8(\text{PET}_3)_2\text{Cl}_4]$ in which the PET_3 ligands preferentially bind the osmium atoms (see Figure 6).

The hexaphosphine clusters were analyzed in solution by ³¹P NMR spectroscopy, indicating marked differences between phosphorus atoms bound to chemically distinct metal sites. The spectrum of the $[\text{Re}_6\text{Se}_8(\text{PET}_3)_6]^{2+}$ cluster in CDCl_3 displays a single resonance located at -31.3 ppm.^{12a} As shown in Figure

(29) Thus, for example, the mass spectra rule out the possibility that the compound formulated as $\text{Cs}_3\text{Re}_5\text{OsSe}_8\text{Cl}_6$ might actually contain a 1:1 ratio of $[\text{Re}_6\text{Se}_8\text{Cl}_6]^{4-}$ and $[\text{Re}_4\text{Os}_2\text{Se}_8\text{Cl}_6]^{2-}$ clusters, a situation which would not necessarily be distinguishable by crystallography alone. See: (a) Mitchell, J. F.; Burdett, J. K.; Keane, P. M.; Ibers, J. A.; DeGroot, D. C.; Hogan, T. P.; Schindler, J. L.; Kannewurf, C. R. *J. Solid State Chem.* **1992**, *99*, 103. (b) Mironov, Y. V.; Cody, J. A.; Albrecht-Schmitt, T. E.; Ibers, J. A. *J. Am. Chem. Soc.* **1997**, *119*, 493.

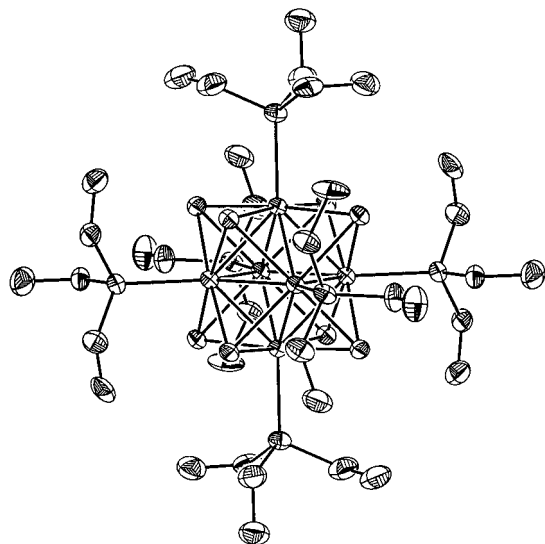
(30) In reactions attempting dimensional reduction by substitution of Ru^{IV} for Re^{III} , we obtained a compound isostructural with $\text{Cs}_3\text{Re}_5\text{OsSe}_8\text{Cl}_6$. Ion exchange yielded crystals of the Bu_4N^+ salt suitable for X-ray analysis; mass spectrometry identified the compound as $(\text{Bu}_4\text{N})_3[\text{Re}_6\text{Se}_7\text{Cl}_7]$.

(31) Yaghi, O. M.; Scott, M. J.; Holm, R. H. *Inorg. Chem.* **1992**, *31*, 4778.

(32) (a) Uriel, S.; Boubekeur, K.; Batail, P.; Orduna, J.; Canadell, E. *Inorg. Chem.* **1995**, *34*, 5307. (b) Uriel, S.; Boubekeur, K.; Batail, P.; Orduna, J. *Angew. Chem., Int. Ed. Engl.* **1996**, *35*, 1544. (c) Decker, A.; Simon, F.; Boubekeur, K.; Fenske, D.; Batail, P. *Z. Anorg. Allg. Chem.* **2000**, *626*, 309. (d) Uriel, S.; Boubekeur, K.; Batail, P.; Orduna, J.; Perrin, A. *New J. Chem.* **2001**, *25*, 737.

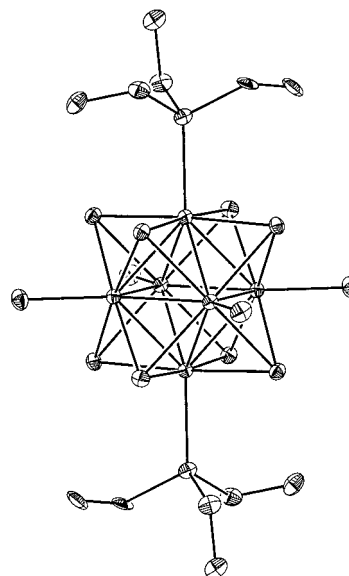
Table 7. Selected Mean Interatomic Distances (Å) and Angles (deg) for the Clusters in [Re₆Se₈(PEt₃)₆](BF₄)₂·2CHCl₃,^{12a} [Re₅OsSe₈(PEt₃)₆]Cl₃·3CH₃CN (7·3CH₃CN), and [Re₄Os₂Se₈(PEt₃)₆]Cl₄·2CH₃CN (8·2CH₃CN)^a

	[Re ₆ Se ₈ (PEt ₃) ₆] ²⁺	[Re ₅ OsSe ₈ (PEt ₃) ₆] ³⁺	[Re ₄ Os ₂ Se ₈ (PEt ₃) ₆] ⁴⁺
M–M	2.646(2)	2.645(6)	2.648(10)
M–Se	2.516(8)	2.509(8)	2.506(6)
M–P	2.479(1)	2.472(10)	2.470(2)
M–Se–M	63.4(1)	63.6(2)	63.8(3)
M–M–P	135.0(13)	135(2)	135(3)
Se–M–Se	89.9(2)	89.9(4)	89.9(3)
	176.4(4)	176.3(3)	176.1(3)
Se–M–P	92.1(13)	92(2)	92(2)

^a M = Re or Os.**Figure 5.** Structure of the [Re₄Os₂Se₈(PEt₃)₆]⁴⁺ cluster in 8·2CH₃CN. Thermal ellipsoids are shown at the 50% probability level, and hydrogen atoms are omitted for clarity. The cluster resides on a crystallographic inversion center.

7, substitution of Os^{IV} for Re^{III} results in resonances that are shifted considerably downfield owing to a decrease in electron density at the phosphorus atoms. For [Re₅OsSe₈(PEt₃)₆]³⁺, the 1:4:1 ratio of peaks is consistent with the C_{4v} symmetry of the cluster core. In addition, the line widths are sufficiently narrow that some splitting patterns are resolved. The complicated environment of each P atom makes specific assignment of splittings difficult; however, on the basis of the similarity in the splitting patterns of the two resonances furthest upfield, we propose that, as might be expected, these arise from P atoms bound to Re^{III}, while the resonance furthest downfield then corresponds to the P atom bound to Os^{IV}. Two sets of peaks are evident in the spectrum of [Re₄Os₂Se₈(PEt₃)₆]⁴⁺: one set displaying a 1:1:1 ratio consistent with the C_{2v} core symmetry of the cis isomer and another exhibiting a 1:2 ratio consistent with the D_{4h} core symmetry of the trans isomer. The relative peak areas further indicate that the trans isomer constitutes approximately 55% of the mixture. Since the ligand substitution was affected in high yield and the cluster cores are not likely to isomerize at low temperatures, it can be inferred that a similar ratio arose from the solid-state reaction producing Cs₂Re₄Os₂Se₈Cl₆.

Redox Properties. Halide-terminated clusters featuring M₆Q₈-type cores with 24 metal-based valence electrons are frequently characterized by a single reversible one-electron oxidation event.^{5b,12h–j,33} Conformably, the cyclic voltammogram of the already oxidized cluster salt (Bu₄N)₃[Re₆Se₈Cl₆] in acetonitrile displays a [Re₆Se₈Cl₆]^{3–/4–} couple centered at E_{1/2} = –0.176 V (ΔE_p = 65 mV) versus Cp₂Fe/Cp₂Fe⁺. As shown in Figure

**Figure 6.** Structure of the site-differentiated cluster trans,trans-[Re₄Os₂Se₈(PEt₃)₂Cl₄]. Thermal ellipsoids are shown at the 50% probability level, and hydrogen atoms are omitted for clarity. The cluster resides on a crystallographic inversion center. Metal atoms are not disordered in the crystal structure: chloride and triethylphosphine ligands are bound to Re and Os atoms, respectively. Selected mean distances (Å) and angles (deg) are as follows: Re–Re 2.616(1), Re–Os 2.640(3), Re–Se 2.514(8), Os–Se 2.489(5), Re–Cl 2.387(5), Os–P 2.430, Re–Re–Re 90.0(1), Re–Os–Re 59.4(1) and 89.0(1), Re–Re–Os 60.3(1), Os–Re–Os 91.0, Re–Se–Re 62.7(1), Re–Se–Os 63.7(2), Se–Re–Se 89.9(13) and 175.8(4), Se–Os–Se 89.9(6) and 175.9(1), Se–Re–Cl 92.1(7), Se–Os–P 92(2).

8, this electrochemical oxidation becomes increasingly more difficult with each substitution of an Os^{IV} center for a Re^{III} center. Thus, the [Re₅OsSe₈Cl₆]^{2–/3–} couple occurs at E_{1/2} = +0.559 V (ΔE_p = 62 mV), while [Re₄Os₂Se₈Cl₆]^{2–} begins to oxidize irreversibly only at approximately +1.1 V. In addition, it appears that reductive decomposition becomes more facile with decreasing negative charge of the cluster, since irreversible reduction processes (not shown) shift to successively higher potentials.

The cyclic voltammograms of the analogous triethylphosphine ligated clusters are displayed in Figure 9 and reveal similar trends with respect to osmium incorporation. In acetonitrile, the compound [Re₆Se₈(PEt₃)₆]I₂ exhibits an oxidation wave corre-

- (33) (a) Maverick, A. W.; Najdzionek, J. S.; MacKenzie, D.; Nocera, D. G.; Gray, H. B. *J. Am. Chem. Soc.* **1983**, *105*, 1878. (b) Ebihara, M.; Toriumi, K.; Saito, K. *Inorg. Chem.* **1988**, *27*, 13. (c) Barnard, P. A.; Sun, I.-W.; Hussey, C. L. *Inorg. Chem.* **1990**, *29*, 3670. (d) Mussell, R. D.; Nocera, D. G. *Inorg. Chem.* **1990**, *29*, 3711. (e) Ebihara, M.; Isobe, K.; Sasaki, Y.; Saito, K. *Inorg. Chem.* **1992**, *31*, 1644. (f) Gabriel, J.-C.; Boubekour, K.; Batail, P. *Inorg. Chem.* **1993**, *32*, 2894. (g) Ebihara, M.; Toriumi, K.; Sasaki, Y.; Saito, K. *Gazz. Chim. Ital.* **1995**, *125*, 87.

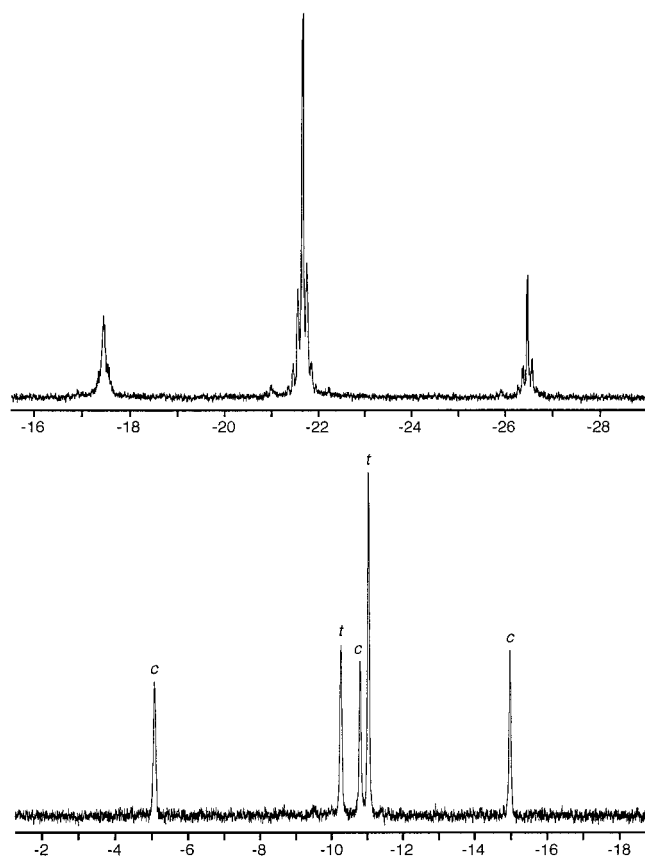


Figure 7. ^{31}P NMR spectra of $[\text{Re}_5\text{OsSe}_8(\text{PEt}_3)_6]\text{Cl}_3$ in CD_3CN (top) and $[\text{Re}_4\text{Os}_2\text{Se}_8(\text{PEt}_3)_6](\text{I}_3)_4$ in $(\text{CD}_3)_2\text{SO}$ (bottom). Proportions between peak integrations are 1.00:4.08:1.01 for $[\text{Re}_5\text{OsSe}_8(\text{PEt}_3)_6]^{3+}$, 1.00:1.00:1.00 for *cis*- $[\text{Re}_4\text{Os}_2\text{Se}_8(\text{PEt}_3)_6]^{4+}$ (peaks labeled with a “c”), and 1.18:2.28 for *trans*- $[\text{Re}_4\text{Os}_2\text{Se}_8(\text{PEt}_3)_6]^{4+}$ (peaks labeled with a “t”). For the latter species, this indicates a *cis*:*trans* ratio of approximately 1:1.16.

sponding to a $[\text{Re}_6\text{Se}_8(\text{PEt}_3)_6]^{2+/3+}$ couple at $E_{1/2} = +0.675$ V ($\Delta E_p = 56$ mV) versus $\text{Cp}_2\text{Fe}/\text{Cp}_2\text{Fe}^+$, as well as a reduction wave corresponding to a $[\text{Re}_6\text{Se}_8(\text{PEt}_3)_6]^{2+/1+}$ couple at $E_{1/2} = -1.905$ V ($\Delta E_p = 64$ mV). With +2 overall charge, it is of little surprise that oxidation of the cluster occurs at a much more positive potential than observed for $[\text{Re}_6\text{Se}_8\text{Cl}_6]^{4-}$ (see Figure 8). Upon substitution of an Os^{IV} center for a Re^{III} center, the reversible oxidation wave is lost, the reduction wave, now corresponding to a $[\text{Re}_5\text{OsSe}_8(\text{PEt}_3)_6]^{3+/2+}$ couple, is shifted to $E_{1/2} = -1.045$ V ($\Delta E_p = 67$ mV), and a second reduction wave associated with a $[\text{Re}_5\text{OsSe}_8(\text{PEt}_3)_6]^{2+/+}$ couple appears at $E_{1/2} = -1.622$ V ($\Delta E_p = 63$ mV). The voltammogram for $[\text{Re}_4\text{Os}_2\text{Se}_8(\text{PEt}_3)_6](\text{I}_3)_4$ (**8**) is complicated by the presence of two distinct isomers of the dioxmium cluster. Three reduction waves are now evident, centered at $E_{1/2} = -0.527$ V ($\Delta E_p = 62$ mV), -0.911 V ($\Delta E_p = 65$ mV), and -1.532 V ($\Delta E_p = 72$ mV), with the second wave being somewhat smaller than the other two. On the basis of the relative ratio of isomers observed in the ^{31}P NMR spectrum of the sample (Figure 7, lower), the smaller reduction wave at -0.911 V is assigned to the *cis* isomer, while the other two waves are assigned to the *trans* isomer. The clusters are stable up to approximately +0.5 V, but this portion of the measurement is obscured by redox chemistry of the I_3^- counterion (not shown in Figure 9).

Consistent with the preceding assignments, the ^{31}P NMR spectrum of $[\text{Re}_4\text{Os}_2\text{Se}_8(\text{PEt}_3)_6]\text{Cl}_4$ (isolated as a precursor to compound **8**) in acetonitrile shows a gradual loss of intensity in the resonances corresponding to the *trans* isomer, until, after 2 days of standing in air, the peaks are nearly immeasurable.

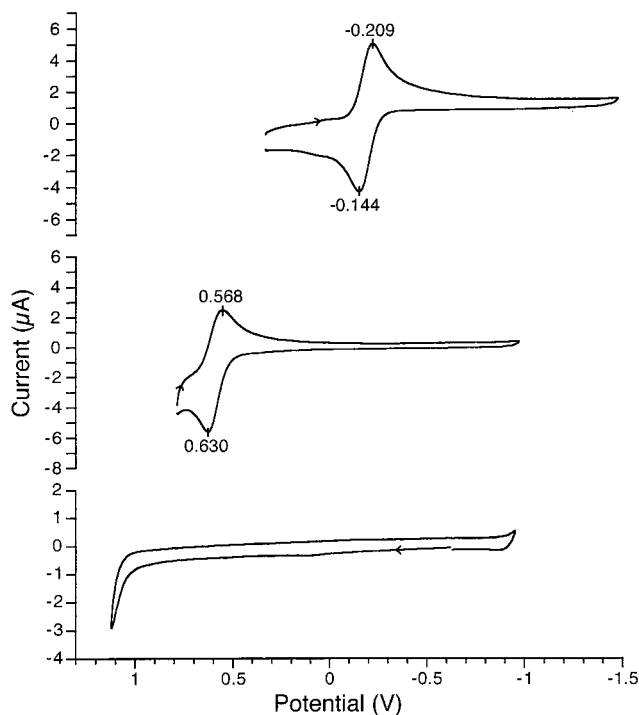


Figure 8. Cyclic voltammograms for $(\text{Bu}_4\text{N})_3[\text{Re}_6\text{Se}_8\text{Cl}_6]$ (top), $(\text{Bu}_4\text{N})_3[\text{Re}_5\text{OsSe}_8\text{Cl}_6]$ (middle), and $(\text{Bu}_4\text{N})_2[\text{Re}_4\text{Os}_2\text{Se}_8\text{Cl}_6]$ (bottom) in acetonitrile. Potentials are reported versus $\text{Cp}_2\text{Fe}/\text{Cp}_2\text{Fe}^+$.

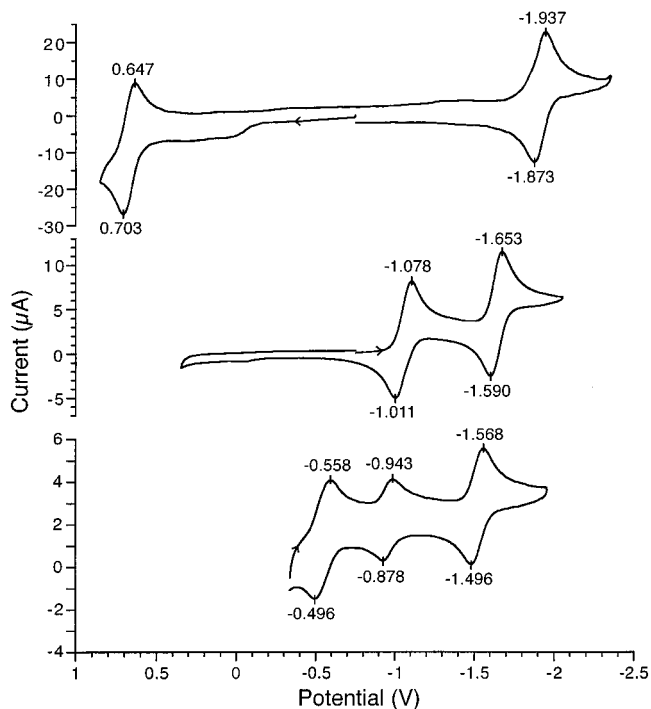


Figure 9. Cyclic voltammograms for $[\text{Re}_6\text{Se}_8(\text{PEt}_3)_6]\text{I}_2$ (top) and $[\text{Re}_5\text{OsSe}_8(\text{PEt}_3)_6]\text{Cl}_3$ (middle) in acetonitrile and for $[\text{Re}_4\text{Os}_2\text{Se}_8(\text{PEt}_3)_6](\text{I}_3)_4$ (bottom) in DMSO. Potentials are reported versus $\text{Cp}_2\text{Fe}/\text{Cp}_2\text{Fe}^+$.

In contrast, the peaks associated with the *cis* isomer remain undiminished. Thus, it appears that the *trans* isomer, having a more accessible reduction wave at -0.527 V, is slowly reduced to give a paramagnetic species whose NMR resonances are then no longer observed. If this interpretation is correct, it may prove possible to separate the two isomers on the basis of the expected differences in solubility of the 25-electron *trans*- $[\text{Re}_4\text{Os}_2\text{Se}_8(\text{PEt}_3)_6]^{3+}$ cluster and the 24-electron *cis*- $[\text{Re}_4\text{Os}_2\text{Se}_8(\text{PEt}_3)_6]^{4+}$ cluster. Replacement of the chloride counteranions with I_3^- ions

provides a sufficiently oxidizing environment that both clusters maintain their 24-electron states in solutions of compound **8**. Reduction beyond 24 metal-based valence electrons is unusual for M₆Q₈-type clusters of second or third row transition metals.^{33aef} To our knowledge, the only prior evidence for the existence of hexarhenium clusters with more than 24 electrons consists of the observation of a quasireversible reduction wave in the cyclic voltammogram of an acetonitrile solution of (Bu₄N)[Re₆S₅Cl₉].^{33f} The rarity of such accessible reduction chemistry therefore invites further study of the phosphine ligated clusters reported here.

Electronic Structures. To probe the effects of osmium incorporation on the frontier molecular orbitals, electronic structure calculations were performed for the clusters [Re_{6-n}Os_nSe₈Cl₆]⁽⁴⁻ⁿ⁾⁻ (*n* = 0–2) using DFT. Idealized geometries based on the crystal structures of Tl₅Re₆Se₈Cl₇,^{5a} 5•2Et₂O, and **6** were assumed. In each case, the calculations showed the highest occupied orbitals to be quite closely spaced, with the eleven highest occupied orbitals spread over no more than 0.5 eV. While these are traditionally described as metal–metal-bonding orbitals on the basis of extended Hückel calculations,³⁴ our results agree with previous DFT studies on related clusters,³⁵ which suggest that several of the orbitals are primarily ligand in character. In addition, the clusters all possess a HOMO–LUMO gap of at least 3.0 eV and LUMOs that are metal–metal antibonding in character. The frontier orbitals for each cluster are similar, with slight perturbations as a result of osmium incorporation; however, their close energy grouping allows even these small perturbations to alter the orbital ordering. In the osmium-containing clusters, the uppermost occupied orbitals are polarized away from the osmium atom(s), while the lowest energy unoccupied orbitals are polarized toward the osmium atom(s). The effect is illustrated in Figure 10, which shows the LUMO and the two highest occupied orbitals for [Re₅OsSe₈Cl₆]³⁻. However, lower energy occupied orbitals are significantly polarized toward the osmium atom, such that, overall, it has approximately 1.1 electrons more than the opposite rhenium atom. This results in a net electric dipole of 0.74 D toward the osmium atom rather than the 22.3 D dipole away from the osmium atom that results from a formal model with Re³⁺ and Os⁴⁺ ions.

The DFT calculations also provide an opportunity for comparing the relative stabilities of the two isomers of [Re₄Os₂Se₈Cl₆]²⁻. Here, our results show the trans isomer to be 4.5 kcal/mol more stable than the cis isomer. Imposing a Boltzmann distribution on the two states then implies that 65% of the clusters should adopt the trans geometry at the synthesis temperature of 875 °C. The ³¹P NMR spectrum of [Re₄Os₂Se₈(PEt₃)₆]⁴⁺ (Figure 7, lower) indicates that 55% of the clusters in the empirical mixture adopt the trans configuration. This percentage suggests an energy difference of 3.5 kcal/mol between the isomers, in reasonable agreement with the calculations. Significantly, the actual difference in energy is large enough to affect which geometry comprises the major product: with no energy difference between isomers, one would expect 80% of the clusters to adopt the cis geometry.

Metal-Selective Reactivity. It is anticipated that the electronic differences between the rhenium and osmium sites in the mixed-

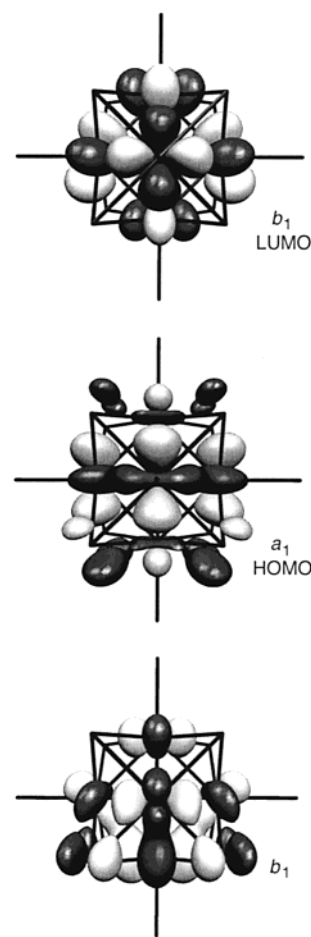


Figure 10. Depictions of the frontier orbitals of the [Re₅OsSe₈Cl₆]³⁻ cluster, as calculated using DFT. The view is down a Re–Cl bond, and the osmium atom is located at the top of the cluster. The HOMO–LUMO separation is 3.4 eV.

metal clusters will lead to metal-selective reactivity. Indeed, the DFT calculations indicate distinct differences in the Os–Cl and Re–Cl bond strengths in the clusters (as reflected in the computed natural bond orders). An initial demonstration of how this can affect their reactivity is provided with the synthesis of trans,trans-[Re₄Os₂Se₈(PEt₃)₂Cl₄] (**9**), wherein PEt₃ ligands preferentially bind the osmium centers (see Figure 6). Several aspects of the crystal structure of **9** indicate the inadequacy of a model employing disordered metal atoms. The thermal parameters of the metal atoms bound to P atoms are 0.012 Å² in such a model, compared with 0.014 Å² for those bound to Cl atoms, whereas localizing the osmium atoms on the phosphorus-bound sites equalizes the thermal parameters. Furthermore, certain of the mean bond distances (listed in the legend of Figure 6) are markedly different: the Re–Re distances are 0.026 Å shorter than the Re–Os distances, while the Re–Se distances are 0.025 Å longer than the Os–Se distances. Finally, replacing the disordered model with the ordered one brings about an improvement in wR₂ from 0.0922 to 0.0917. Since only one electron out of 462 is being moved with such a change, a shift in wR₂ of this magnitude is significant and, when considered together with the foregoing observations, suggests that the ordered model is correct. Further exploring the influences of the different metal sites on the reactivity of these and related mixed-metal clusters poses a subject for future study.

Outlook

Applied in conjunction with core anion substitution and/or standard dimensional reduction, the heterometal substitution

- (34) (a) Hughbanks, T.; Hoffmann, R. *J. Am. Chem. Soc.* **1983**, *105*, 1150. (b) Hughbanks, T. *Prog. Solid State Chem.* **1989**, *19*, 329. (c) Lin, Z.; Williams, I. D. *Polyhedron* **1996**, *15*, 3277.
- (35) (a) Robinson, L. M.; Bain, R. L.; Shriver, D. F.; Ellis, D. E. *Inorg. Chem.* **1995**, *34*, 5588. (b) Arratia-Perez, R.; Hernandez-Acevedo, L. *J. Chem. Phys.* **1999**, *110*, 2529. (c) Arratia-Perez, R.; Hernandez-Acevedo, L. *J. Chem. Phys.* **1999**, *111*, 168.

technique demonstrated here is potentially capable of supplying many new soluble cluster species. With recognition that the preferred electron count may differ or even vary, the method should extend to other parent frameworks with face-capped octahedral cluster cores, such as Mo_6Q_8 (Q = S, Se, Te) and M_6X_{12} (M = Mo, W; X = Cl, Br, I).^{7,11} It should further extend to frameworks comprised of cluster cores with other geometries, such as Re_3X_9 (X = Cl, Br, I), $\text{Nb}_6\text{Cl}_{14}$, and $\text{Zr}_6\text{ZCl}_{12+z}$.^{11,16} Substitutions employing metals with fewer valence electrons than the parent metal (e.g., Mo or W for Re) are also feasible and would be expected to decrease the charge of the cluster core. As well as aiding in the development of an understanding of how heterometal substitution influences the physical properties and reactivity of a cluster, it is hoped that the technique will be of value in the numerous areas of investigation already involving homometallic clusters.^{12,36}

Acknowledgment. This research was funded by the Research Corp., the Camille and Henry Dreyfus Foundation, NSF Grant No. CHE-0072691, and the University of California, Berkeley, CA. We thank Atofina Chemical Inc. for providing E.G.T. with a fellowship, N. R. M. Crawford for assistance with

the DFT calculations, Dr. F. Hollander for helpful discussions, and Prof. A. M. Stacy for use of the X-ray powder diffractometer.

Supporting Information Available: An X-ray crystallographic file (CIF) for the compounds listed in Tables 1 and 2, including tables of crystal and refinement data, atomic positional and thermal parameters, and interatomic distances and angles, and depictions of the isomers of the cluster cores enumerated in Table 5. This material is available free of charge via the Internet at <http://pubs.acs.org>.

IC010867D

- (36) Selected references: (a) Gray, H. B.; Maverick, A. W. *Science* **1981**, *214*, 1201. (b) Ekman, M. E.; Anderegg, J. W.; Schrader, G. L. *J. Catal.* **1989**, *117*, 246. (c) Qi, R. Y.; Corbett, J. D. *Inorg. Chem.* **1994**, *33*, 5727. (d) Golden, J. H.; Deng, H. B.; DiSalvo, F. J.; Fréchet, J. M. J.; Thompson, P. M. *Science* **1995**, *268*, 1463. (e) Hilsenbeck, S. J.; McCarley, R. E.; Goldman, A. I. *Chem. Mater.* **1998**, *10*, 125. (f) Prokopuk, N.; Shriver, D. F. *Chem. Mater.* **1999**, *11*, 1230. (g) Deluzet, A.; Batail, P.; Misaki, Y.; Auban-Senzier, P.; Canadell, E. *Adv. Mater.* **2000**, *12*, 436. (h) Jin, S.; Venkataraman, D.; DiSalvo, F. J. *Inorg. Chem.* **2000**, *39*, 2747. (i) Mironov, Y. V.; Virovets, A. V.; Naumov, N. G.; Ikorskii, V. N.; Fedorov, V. E. *Chem. Eur. J.* **2000**, *6*, 1361. (j) Xie, X. B.; Jones, J. N.; Hughbanks, T. *Inorg. Chem.* **2001**, *40*, 522.